Microbiology Spectrum
American Society for Microbiology Press

Transposable Phage Mu

RASIKA M. HARSHEY
Department of Molecular Biosciences, Institute of Cellular and Molecular Biology, University of Texas at Austin, Austin, TX 78712

ABSTRACT Transposable phage Mu has played a major role in elucidating the mechanism of movement of mobile DNA elements. The high efficiency of Mu transposition has facilitated a detailed biochemical dissection of the reaction mechanism, as well as of protein and DNA elements that regulate transpososome assembly and function. The deduced phosphotransfer mechanism involves in-line orientation of metal ion-activated hydroxyl groups for nucleophilic attack on reactive diester bonds, a mechanism that appears to be used by all transposable elements examined to date. A crystal structure of the Mu transpososome is available. Mu differs from all other transposable elements in encoding unique adaptations that promote its viral lifestyle. These adaptations include multiple DNA (enhancer, SGS) and protein (MuB, HU, IHF) elements that enable efficient Mu end synapsis, efficient target capture, low target specificity, immunity to transposition near or into itself, and efficient mechanisms for recruiting host repair and replication machineries to resolve transposition intermediates. MuB has multiple functions, including target capture and immunity. The SGS element promotes gyrase-mediated Mu end synapsis, and the enhancer, aided by HU and IHF, participates in directing a unique topological architecture of the Mu synapse. The function of these DNA and protein elements is important during both lysogenic and lytic phases. Enhancer properties have been exploited in the design of mini-Mu vectors for genetic engineering. Mu ends assembled into active transpososomes have been delivered directly into bacterial, yeast, and human genomes, where they integrate efficiently, and may prove useful for gene therapy.

INTRODUCTION

Transposable phage Mu has played a historic role in the development of the mobile DNA element field (1). The very first paper that christened this phage after its **mu**tator properties (2) also drew attention to its ability to suppress the phenotypic expression of genes, and suggested that Mu resembled the "controlling elements" postulated by Barbara McClintock to regulate the mosaic color patterns of maize seeds (3). This bold postulate inspired equally insightful early experiments aimed at investigating its mobile properties (4, 5), and led to an influential model for transposition (6), which correctly predicted the cutting and joining steps of the Mu transposition reaction and their attendant DNA rearrangements. The high efficiency of the Mu reaction was responsible for the development of the first *in vitro* transposition system (7), which was critical for dissecting reaction chemistry as well as the function of several participating proteins (see references 8 and 9). This article focuses on the major developments in Mu transposition since this topic was last reviewed in Mobile DNA II, providing background information as necessary (9).

ONE TRANSPOSITION MECHANISM, TWO PATHWAYS FOR PRODUCT RESOLUTION

Mechanism

The mechanism of Mu transposition has been deciphered *in vitro* on both supercoiled and oligonucleotide substrates (10). Figure 1 shows transposition events in the context of *in vivo* substrates. Mu transposition has two distinct phases, which differ in donor substrate configuration and in the fate of the transposition products (8). During the infection phase, the Mu DNA injected into

Received: 5 March 2014, **Accepted:** 14 June 2014,
Published: ••••••
Editors: Mick Chandler, Université Paul Sabatier, Toulouse, France, and Nancy Craig, Johns Hopkins University, Baltimore, MD
Citation: Harshey RM. 2014. Transposable phage Mu. *Microbiol Spectrum* 2(5):MDNA3-0007-2014. doi:10.1128/microbiolspec.MDNA3-0007-2014.
Correspondence: Rasika Harshey, rasika@uts.cc.utexas.edu

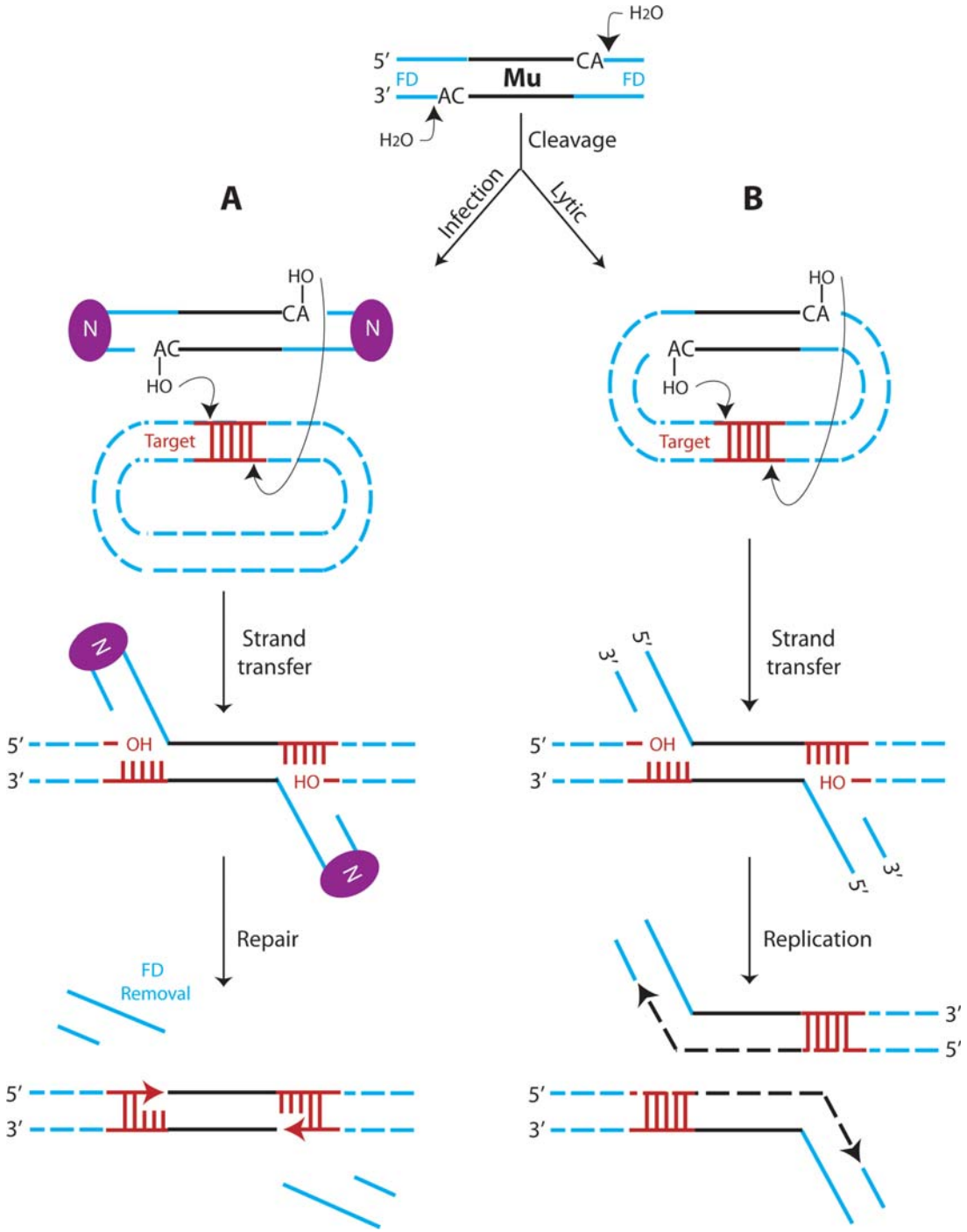

FIGURE 1 One transposition mechanism, two pathways for resolution of the ST intermediate. The chemical steps of cleavage and ST are the same in both the infection and lytic phases of transposition. **(A)** In the infection phase, the linear donor Mu genome is converted into a noncovalently closed circle, joined by the MuN protein (purple ovals, ends shown unjoined for clarity); *E. coli* genome is the target. The ST intermediate formed during intermolecular transposition is resolved by removal of the FD, and repair of the 5-bp gaps in the target by limited replication at the host–Mu junction. **(B)** In the lytic phase, Mu is part of the covalently closed circular *E. coli* genome. The ST intermediate formed during intramolecular transposition is resolved by replication across Mu. doi:10.1128/microbiolspec.MDNA3-0007-2014.f1

cells has a peculiar structure. This DNA is linear in the phage heads, and flanked by non-Mu host DNA acquired during packaging of integrated Mu replicas during the lytic cycle in a prior host. The number of base pairs of the host sequences that flank the left, or L, end of Mu is 60 to 150 kb, and 0.5 to 3 kb flank the right, or R, end (8). An injected phage protein N binds to the tip of the flanking DNA (FD), protecting the open ends from degradation while also converting the linear genome into a noncovalently closed supercoiled circle prior to integration into the host chromosome (drawn linear for clarity in Fig. 1A) (11, 12, 13). (Non-Mu flanking DNA is referred to as FD herein, irrespective of whether the donor substrate is phage, prophage, plasmid, or oligonucleotide.) During the lytic phase, Mu is part of a large covalently closed circular host genome (Fig. 1B). Thus, the donor Mu DNA configuration in the infection phase is different from that during the lytic phase. In both phases, the mechanism of Mu transposition is the same.

The transposase MuA initially generates a pair of water-mediated endonucleolytic cleavages on specific Mu–host phosphodiester bonds, producing 3′-OH nicks at Mu DNA ends (Fig. 1, Cleavage). In the subsequent strand-transfer (ST) step, the 3′-OH ends directly attack phosphodiester bonds in the target DNA spaced 5 bp apart; this reaction is intermolecular in the infection phase (Fig. 1A) and intramolecular in the lytic phase (Fig. 1B). Mu ends join to 5′-Ps in the target, leaving 3′-OH nicks on the target. The MuB protein is essential for the efficient capture of the target, but plays critical roles at all stages of transposition by allosterically activating MuA (see below) (9). The cleavage and ST reactions, also called phosphoryl transfer reactions (14), are common to other DNA transposition systems including retroviral integration (15). These reactions take place within the same active site of MuA, which contains a structurally conserved "DDE" domain, so named for the three Mg^{2+}-binding carboxylate residues found in other transposases and recombinases (16). Divalent metal ions coordinated by the DDE residues are proposed to activate hydroxyl groups for nucleophilic attack on the reactive phosphodiester bonds in both steps of transposition (10, 17). These reactions proceed via bimolecular nucleophilic substitution (S_N2), a mechanism shared by metal-dependent nucleotidyl transferases and some nucleases (18, 19, 20). Crystal structures of the HIV-related prototype foamy virus (PFV) retroviral integrase assemblies (intasomes), whose phosphotransfer mechanism is similar to Mu, validate the S_N2 mechanism (21, 22, 23).

Two pathways for product resolution

Post-transposition, the branched ST intermediate product must be resolved (Fig. 1A and B). During the infection phase, the intermediate is resolved by FD removal/degradation and repair of the 5-bp gaps in the target by limited DNA replication, generating a simple insertion of Mu in the *Escherichia coli* genome. During the lytic phase, the intermediate is resolved by target-primed replication across the entire Mu genome. These product resolution pathways are referred to as repair or replication pathways herein. The replication pathway has been reconstituted *in vitro* and studied in some detail. The repair pathway has been studied only *in vivo*, and is in the early stages of characterization. The known steps in both pathways are described later.

DISINTEGRATION

A chemical reversal of the transposition/integration reaction is called disintegration. In such a reaction, the 3′-OHs created on the target DNA after ST would attack the phosphodiester bonds formed at the transposon-target junction during the forward reaction (Fig. 2A, red arrows), restoring the original target configuration and releasing the cleaved donor. Disintegration is normally not observed, despite the fact that the forward and reverse reactions are isoenergetic. The reverse reaction can, however, be demonstrated *in vitro* using altered substrates and reaction conditions. Reversal of ST was first described for HIV-1 integrase on oligonucleotide ST substrates (24), and subsequently reproduced in other systems (25, 26, 27, 28). The reported reaction is a pseudo reversal, also called foldback reversal, because the substrates employed resemble a ST joint that has been unpaired and flipped (or folded back), so that the target 3′-OHs attack the transposon-target joint in an unnatural *trans* configuration rather than the normal *cis* configuration, creating hairpin ends on the target (Fig. 2B). The disintegration reaction was also observed for Mu, on both oligonucleotide and plasmid substrates, and required high temperatures or altered metal ions (29, 30). Both true as well as pseudo reversal were observed for Mu (Fig. 2A and B), each showing distinct metal ion specificities indicative of different configurations of the reactive components within the active site. Ca^{2+} ions, which support ST of precleaved ends, also supported true reversal; these ions did not support pseudo reversal, suggesting that the metal ion binding pocket is similar in the forward and the true-reversal reactions, but different in the foldback reaction. When the transpososome was assembled on uncleaved Mu donor substrates, and the

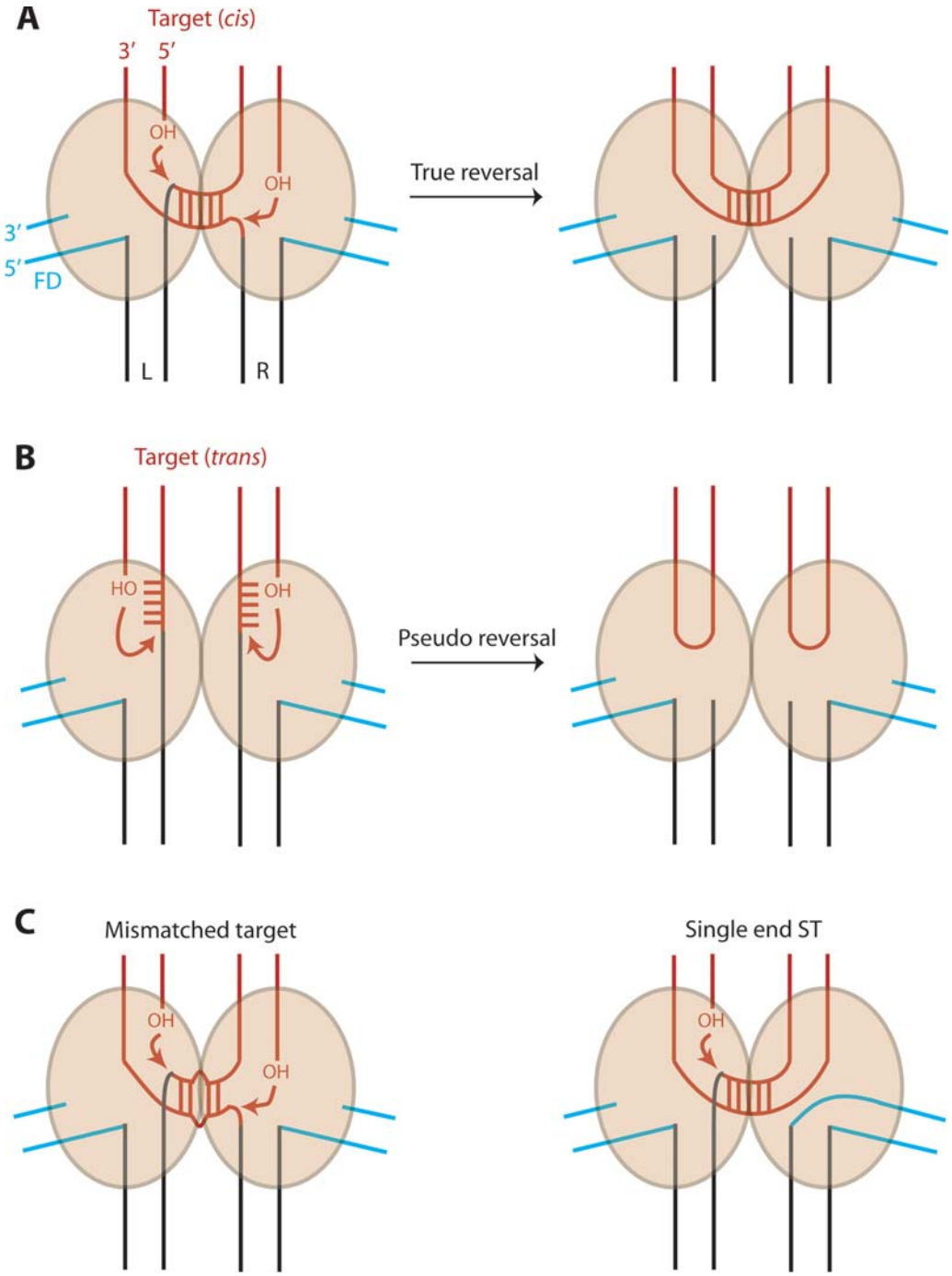

FIGURE 2 Disintegration: true and pseudo reversal. Ovals represent the transposase active sites. **(A)** True reversal refers to restoration of the original target configuration by a *cis* nucleophilic attack of the target 3′-OHs on the target–host junction generated during ST. L and R refer to the left and right ends of Mu. **(B)** In pseudo reversal, the target is rearranged (imagine unpairing the 5 bp in A, and flipping the DNA through 180°), so that the target nucleophiles attack the host–target junction in *trans*, resulting in hairpin products. **(C)** True reversal is more facile if the target carries a mismatch (left) indicated by an unpaired base pair, or if only a single end undergoes ST within the transpososome (right). See text for details. doi:10.1128/microbiolspec.MDNA3-0007-2014.f2

reaction proceeded through the 3′ Mu end cleavage and ST, true reversal required high temperatures (29, 30), suggesting that, in the normal course of events, the reactive groups are rearranged within the ST complex such that reversal is proscribed; high temperatures likely cause conformation changes that restore the pre-ST configuration of the active site (29). The higher stability of the ST complex compared to the cleaved complex (31) is consistent with the notion of structural transitions in the transpososomes (and hence the active sites) as the reaction proceeds forward. True reversal was also observed when mismatched bases were incorporated in the target (Fig. 2C, left), likely because of increased target flexibility around the mismatch, which allows the ST joint to explore normally disfavored spaces that promote reversal (29). Support for the conjecture that the reversal of ST is normally prevented because of misalignment of the reactive groups after ST comes from crystal structures of PFV intasomes captured at various stages of the reaction (32). The viral DNA–target DNA joint was observed to be ejected from the active site after ST, and thus no longer available for reversal (21).

Disintegration has also been observed on plasmid substrates at which only a single Mu end was allowed to undergo cleavage and ST (Fig. 2C, right) (33). Vulnerability of the single-ended joint to reversal is favored in the absence of the transposase-activator protein MuB, revealing a role for MuB in coordinating the configuration of both active sites so as to prevent reversal. On plasmid substrates, where the STs of both Mu ends are highly concerted, high-temperature disintegration (either true or pseudo) was observed at only one of the two ends (29), suggesting that both active sites cannot simultaneously adopt a reversal configuration.

TRANSPOSOSOME ASSEMBLY, ACTIVITY, AND STRUCTURE

Normal versus minimal DNA-protein requirements

Mu transposition requires MuA binding to sites at the left (L) and right (R) ends (also referred to as *att* ends), as well as at an enhancer (E) DNA segment located ~1 kb away from the L end on the Mu genome (Fig. 3A) (9). The L and R ends are asymmetric with respect to orientation and spacing of the three MuA-binding sites at each end (L1–L3 and R1–R3). There are three MuA-binding sites at E as well (O1–O3). Separate regions within MuA bind to the end and enhancer sites (Fig. 3B). Under physiological reaction conditions, transpososome assembly requires that both sets of DNA sites in their native configuration be present on supercoiled Mu donor DNA, along with the *E. coli* protein HU, which binds between L1 and L2 at the L end (Fig. 3A); the *E. coli* IHF protein, which binds between O1 and O2 at E, optimizes assembly. In the presence of the divalent metal ion Mg^{2+}, these components are sufficient for promoting the DNA cleavage reaction. ST requires MuB in addition (Fig. 3C). MuB is an AAA+ ATPase, which binds DNA nonspecifically (9, 34). The ATPase activity of MuB is stimulated by DNA and MuA. MuB not only captures target DNA and delivers it to the transpososome, but also its interactions with MuA optimize all stages of transpososome assembly (Fig. 4) (9, 34, 35, 36).

A minimal transposition system has been established *in vitro*, in which addition of the solvent Me_2SO (dimethyl sulfoxide) allows oligonucleotide substrates encoding only the R1–R2 subsites to undergo efficient pairing, cleavage, and ST by MuA alone, in the absence of DNA supercoiling, the enhancer, the N-terminal enhancer-binding MuA domain Iα, HU, MuB, and the C-terminal MuB/ClpX-binding MuA domain IIIβ (37). These permissive reaction conditions have greatly aided the dissection of the transposition reaction (9).

Assembly, cleavage, strand transfer

The transposase MuA is a monomer in solution and does not assemble into a multimeric form unless bound to Mu ends (9). MuA subunits bound to all six L and R binding sites interact with the enhancer (Fig. 3A), and assemble into a transpososome. In a transpososome built from six MuA subunits, two subunits are loosely held; high salt treatment of the native transpososome yields a stable tetrameric core that is catalytically proficient. Within this tetrameric core, only two subunits, those bound to L1 and R1, catalyze cleavage and ST in *trans*, i.e., the subunit bound to L1 is responsible for catalysis at the R1 end and vice versa. The disintegration reaction also occurs in *trans* (33). Oligonucleotide substrates (R1–R2) also assemble a tetrameric MuA, and also catalyze the reaction in *trans* (9).

A variety of approaches have been used to dissect the configuration of the Mu ends within the two MuA active sites, the role of MuB in coordinating the reaction, and the role of metal ions. The results are summarized below ([i]–[vii]), and can be followed using Fig. 4 as a guide. Reaction chemistry occurs on the strands that end in CA (see Fig. 1), called the transferred strands; the opposite strands are the nontransferred strands. The terminal Mu base pair is designated +1, while the base pair immediately outside on the FD is −1. The role of the enhancer is discussed in a later section.

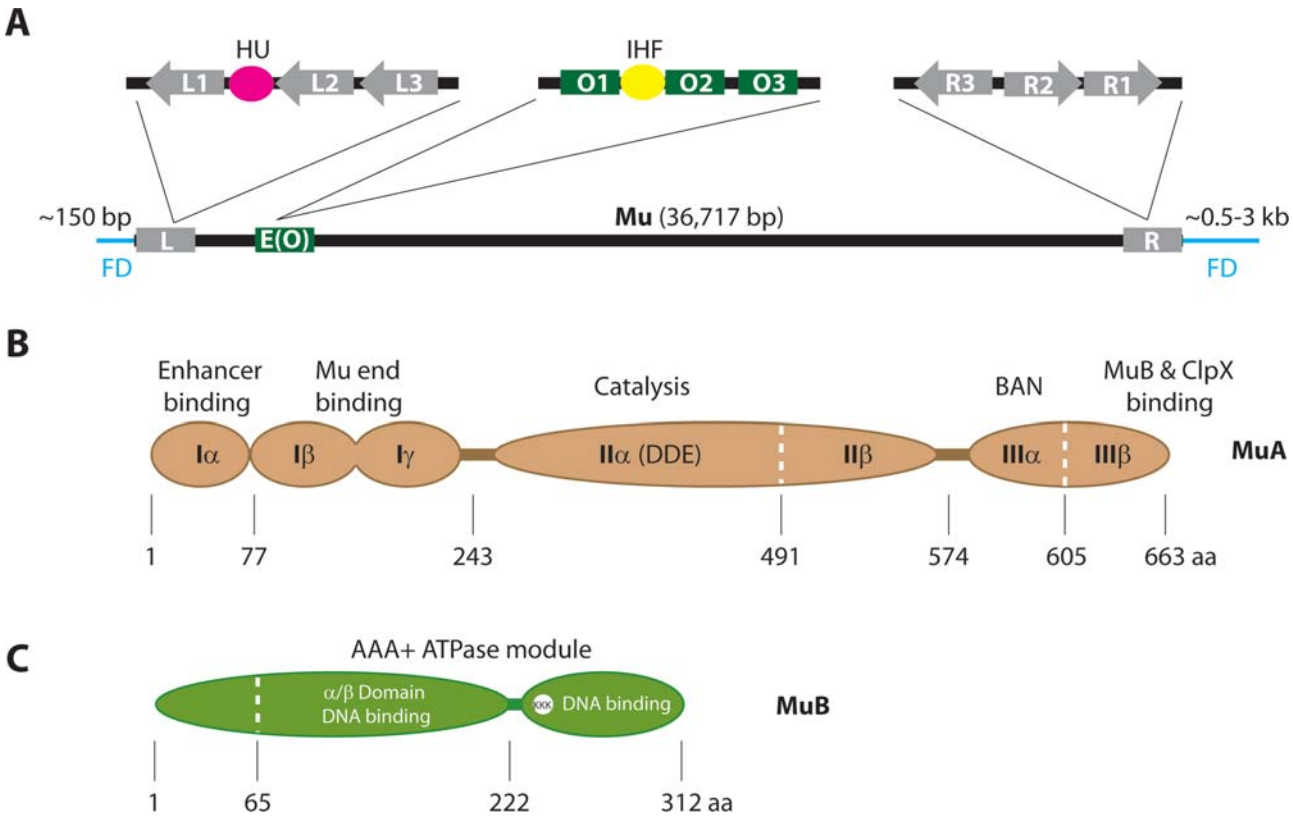

FIGURE 3 DNA and protein requirements for transposition. **(A)** Arrangement of MuA binding sites at the L (L1–L3) and R (R1–R3) ends of the Mu genome, and within the Mu enhancer E (O1–O3). E is positioned closer to the L end on the Mu genome, and is also labeled O because of its dual function as an operator that regulates lysis/lysogeny decision (8). HU and IHF bind within L and E as shown. FD on either side of the Mu genome packaged into virions. **(B)** Domain and subdomain organization of MuA as assigned by partial proteolysis (140). NMR and crystal structures for the individual (except IIIβ) are available (9, 62, 141). The subdomain IIβ was observed in crystal structures (142), while IIIα and IIIβ were delineated by mutagenesis and functional studies (9). BAN stands for DNA-binding and nuclease function (122). See reference 143 for an insertion mutagenesis study across the domains. **(C)** Domain organization of MuB, as assigned by partial proteolysis (144). An NMR structure for the C-terminal domain is available (145). An AAA+ ATPase function spanning residues in both domains was deduced by bioinformatics, and supported by mutagenesis (34). Both domains also contribute to nonspecific DNA binding (9, 34, 35). A patch of positively charged residues (KKK) on the C-terminal domain likely interacts with MuA to trigger ATP hydrolysis (34, 35). The conformation of the hinge region between the domains is exquisitely modulated by ATP, DNA, and A protein, as judged by its sensitivity to proteolysis (146). doi:10.1128/microbiolspec.MDNA3-0007-2014.f3

(i) Initial engagement of Mu ends and stable assembly

The rate-limiting step of Mu transposition is inferred to be a DNA melting event around the cleavage sites, not the subsequent reaction chemistry (37, 38, 39, 40). On supercoiled substrates, the free energy of supercoiling in the DNA outside the Mu ends (FD), but not inside Mu, is used to lower the activation barrier of this rate-limiting step, implying that the Mu ends pair and sequester the supercoils into separate Mu and FD DNA domains, before selectively using supercoiling energy stored in the FD domain (Fig. 4A) (38). The terminal CA dinucleotide, conserved in many transposable elements, including retroviruses (41), appears to be chosen at this position for its flexibility and ease of distortion (42, 43), rather than for its reaction chemistry (40, 43, 44). Mutant termini can assemble an unstable form of the left-end, enhancer and right-end (LER) transpososome (see "Enhancer and transpososome topology"), but fail to promote stable assembly (45). However, mismatched

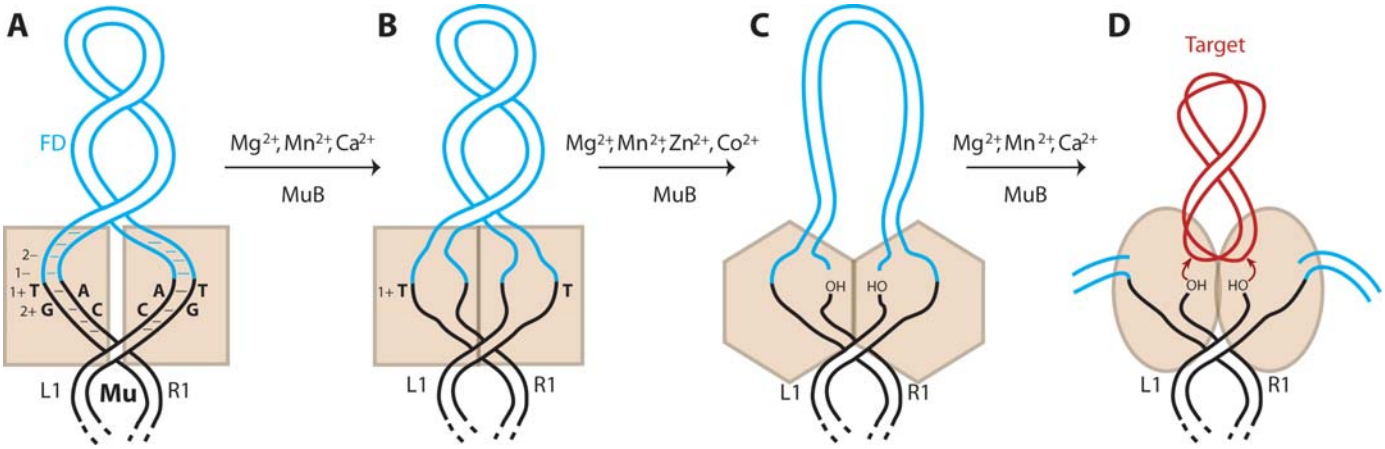

FIGURE 4 DNA–protein transitions with the MuA active sites. **(A)** Terminal base pairs at the Mu ends (L1 and R1 sites) and its adjoining FD are engaged within the MuA active sites (squares). Catalysis is in *trans*, i.e., the MuA subunit bound at R1 engages the L1 terminus and vice versa (9). This complex is not stable, and MuA has not tetramerized (indicated by a separation of the squares). **(B)** After Mu end synapsis, the free energy of supercoiling in the FD domain is used to melt several base pairs around the Mu–FD junction, concomitant with tetramerization of MuA (indicated by contiguous squares) (9). Mismatched substrates will tolerate any nucleotide at the terminal 2 bp, but require T at the +1 position on the nontransferred strand for stable MuA assembly. **(C)** Mismatched termini can cleave adjacent to any nucleotide at the +1 position on the transferred strand. The cleaved complex is more stable, indicated by a shape change to hexagons. **(D)** ST can occur on precleaved substrates even from an abasic site. This complex is the most stable, indicated by a shape change to the ovals. Each stage of transition (A–D) exhibits specific metal ion requirements and is regulated by MuB. See text for details. doi:10.1128/microbiolspec.MDNA3-0007-2014.f4

mutant termini assemble readily (40, 46), indicating that engagement of the melted DNA strands within the active site promotes larger conformational changes that allow MuA subunits to oligomerize into a stable complex (Fig. 4B). Assembly defects at +1 are more severe than those at at +2 or +3, and Mn^{2+} ions suppress these defects, suggesting a role for metal ions in modulating active-site conformation (45). On the nontransferred strand, the +1 T residue is essential for assembly even on mismatched substrates, with the R group at position 5 important for the initial contact but dispensable after cleavage of the transferred strand (Fig. 4B) (40, 46). Fully base-paired substrates require divalent metal ions for assembly (Mg^{2+}, Mn^{2+}, or Ca^{2+}), but this requirement is substantially reduced on substrates with mismatched termini (46), or if the FD strands are not complementary, or are very short, or the substrate is precleaved (37), implying that on fully base-paired substrates metal ions assist in the DNA opening observed around Mu ends (Fig. 4A and B) (39, 45, 47). MuB stimulates assembly on both plasmid and oligonucleotide substrates; the stimulation is independent of the presence of the FD on oligonucleotide substrates (36).

When concentrations of Mu DNA are limited, MuA bound to its end-recognition sites can capture and assemble non-Mu DNA sequences that resemble the Mu sequence; considerable variability in the placement of the MuA binding site with respect to the cleavage site appears to be tolerated by the transposition machinery (48, 49).

(ii) DNA cleavage

As described above, the cleavage reaction is independent of nucleotide sequence when the terminal bases are unpaired. This reaction is also more efficient if the DNA flanking the Mu ends is not base paired (37). The MuA active sites accept hairpin substrates with different "loop" lengths for cleavage (50). Although Mg^{2+} is likely the biologically relevant cation, Mn^{2+} ions support both cleavage and ST in all the transposition systems studied. However, preassembled Mu substrates can be cleaved by Zn^{2+} and Co^{2+} (Fig. 4B and C) (39).

(iii) DNA ST

The wild-type nucleophile for ST is the 3′-OH of the terminal adenosine. However, Mu termini ending in

a dideoxynucleotide allow target DNA hydrolysis by a water nucleophile (44). Remarkably, substrates that terminated with an abasic site, i.e., contained the terminal ribose and its 3′-OH, but were missing the adenine base, promoted efficient ST. Thus, it is not the terminal base, but rather the ribose (and/or the attached 5′-phosphate) that is the critical activating feature of the terminal nucleotide (Fig. 4C). It appears that the presence of the terminal nucleotide prevents the use of inappropriate nucleophiles, and offers an advantage to the attached 3′-OH to serve as the nucleophile.

Precleaved ends will perform ST in the presence of Ca^{2+} (Fig. 4D) (37). A true reversal of ST can also use Ca^{2+} (see "Disintegration"). Since a single active site carries out both cleavage and ST, the differential metal ion selectivity in cleavage (which is not supported by Ca^{2+}) versus ST must reflect either conformational differences between the active sites during the two steps or differences in the way the two distinct nucleophiles are activated.

(iv) Coupling catalysis at the paired ends

The normal transposition reaction is highly concerted at both ends. When only one end carries a mutation in the terminal dinucleotide, stable assembly of both ends is blocked (51). Metal ions and MuB protein influence this tight coupling between the two active sites as judged by situations in which the coupling is lost. For example, both Mn^{2+} ions and MuB suppress the assembly and catalysis defects of mutations at one Mu end (9, 51, 52). So also, hairpin ends react in a concerted manner with Mn^{2+} ions, but only produce single-end ST with Mg^{2+} (50). In the absence of MuB, the presence of FD in only one active site slows the ST of precleaved substrates in both active sites (36). MuB also suppresses mutations of G residues at the +2 position on the bottom strand, influencing the degree of concerted ST activity (46). Thus, MuB influences all steps of transpososome assembly and catalysis. The allosteric effect of MuB is apparently not effected through any specific MuA subunit (53).

(v) FD configuration

As described above, several nucleotides adjacent to the Mu termini on the FD also undergo melting during assembly, and this single-stranded feature of the FD is important for DNA cleavage (Fig. 4B). After cleavage, the FD must be moved away to accommodate the target DNA (Fig. 4D); this is evident in the finding that in the absence of MuB, the presence of the FD in only one active site slowed one or more steps between DNA cleavage and joining in both sites, and that this slow step was not due to a change in the affinity of the transpososome for the target DNA (36). Thus, MuB interaction with MuA coordinates shifting the FD in both active sites, coupling this movement to a conformational change within the transpososome that positions the target DNA for coordinated ST.

(vi) Target capture and DNA conformation

Transpososomes assembled on plasmid donor Mu substrates can capture target DNA even prior to DNA cleavage, i.e., at the stage shown in Fig. 4A (54). Interestingly, on these substrates the terminal MuA binding site L1, but not R1, is required for target capture (47). Transpososomes assembled on R1–R2 oligonucleotide substrates lacking the terminal 3 bp are capable of target DNA capture, indicating that the target-interacting surface of the transpososome can be organized without the Mu-terminal nucleotides (Fig. 4D) (40). A single mismatch in the center of the 5-bp target recognition sequence promotes preferential use of the mismatched target, likely because it gives the target more flexibility for adopting the severely bent target configuration seen in the crystal structure (Fig. 5) (55), a feature found in other transpososome structures as well (21, 56). Given that transposition to nonmismatched sites is suppressed when mismatched sites are available suggests that the transposon–transposase complex samples a large number of potential target sites before ST.

(vii) Plasticity of the active site

As evidenced from the description above, the ability of a variety of DNA end configurations (fully paired, unpaired, hairpin) to be accommodated within the active site, of a variety of metal ions to support different stages of integration and disintegration, and of both half and full target sites to permit disintegration speaks to the remarkable plasticity of the active site (10).

Transpososome structure

Electron microscopy (EM)

The crystal structure of the dimeric Tn5 transposase in complex with DNA provided the earliest glimpse of a transposase active site (57). As first demonstrated for MuA (9), the Tn5 transposase subunits were observed to be arranged in *trans* for catalysis (57), a feature proving to be widespread among mobile elements (22, 58, 59, 60). The structure of a six-subunit Mu transpososome is expected to be more complex than that of a dimeric one. Although the structures of nearly all the individual domains of MuA were determined by nuclear magnetic resonance (NMR) or X-ray methods (Fig. 3B) (9), the

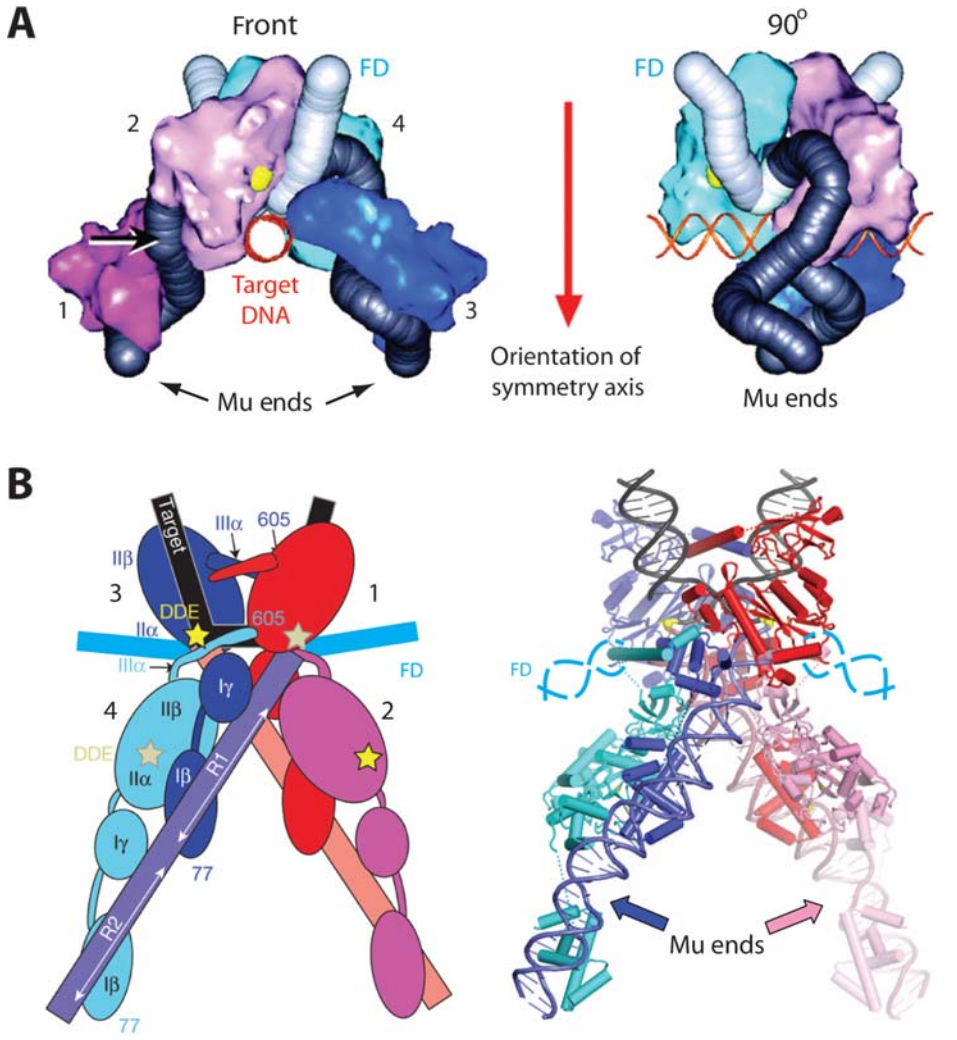

Q1

FIGURE 5 Mu transpososome structures assembled on oligonucleotide substrates. **(A)** Two views of the 3D reconstruction of images of a cleaved MuA tetramer bound to R1 and R2 ends, obtained by scanning transmission electron microscopy at cryotemperatures, combined with electron spectroscopic imaging of the DNA-phosphorus (61). Target DNA is modeled into the structure. Location of Mu ends (black tubes) and FD (gray tubes) is indicated. The image has been modified from the original in order to match the orientation of the X-ray image in B. **(B)** X-ray crystal structure of the Mu transpososome engaged with cleaved R1 and R2 Mu ends joined to target DNA (62). The MuA polypeptide in the crystal structure includes residues 77 to 605; it is missing the regulatory N (Iα)- and C (IIIβ)-terminal domains (see Fig. 3B). Left, schematic illustrating positions of the various MuA domains and DNA segments. Catalytic sites are marked as tan/yellow stars. Right, ribbon drawing, with the scissile phosphate groups shown as yellow spheres. The figure is modified to indicate position of the FD. In the crystal structure, the BAN region in domain IIIα (see Fig. 3B) of the R2-bound subunits (cyan and pink) makes contact with the FD near the Mu–FD junction; this region is associated with a nonspecific endonuclease activity (122). Adapted with permission from the Nature Publishing group. doi:10.1128/microbiolspec.MDNA3-0007-2014.f5

entire complex proved difficult to crystallize. The first three-dimensional image of a tetrameric Mu transpososome assembled on precleaved R1–R2 oligonucleotide substrates was published by Yuan et al. who used scanning transmission electron microscopy (Fig. 5A) (61). Although the resolution of the reconstruction was relatively low (34 Å), it satisfied several biochemical observations, particularly the *trans* arrangement of the

subunits for catalysis. A model of the complex resembled a large V (shown inverted in Fig. 5A), with the only significant protein–protein interactions occurring at the bottom of the V where the catalytic subunits were located, the rest of the complex apparently held together only by DNA–protein interactions. The latter observation was proposed to provide flexibility to the overall complex as it transitioned into increasingly stable states with each step of the reaction. Target DNA was modeled to fit into the cleft of the V in the 3D structure (Fig. 5A). The X-ray structure of the ST transpososome shows the target DNA also accommodated at the bottom, but on the other side of the V cleft (see below).

X-ray crystallography

The crystal structure of the Mu ST transpososome assembled on R1–R2 subsites joined to target DNA is shown in Fig. 5B (62). A truncated version of MuA (residues 77 to 605) was used for assembly (Fig. 3B). Efficient ST of precleaved substrates was achieved by employing a target substrate with a single mismatch, described under "Target capture and DNA conformation" (above). The overall transpososome shape is consistent with the V shape described by scanning EM (Fig. 5A), where protein–protein interactions are mainly between the catalytic subunits at the bottom of the V. As expected, the DDE residues in domain IIα of subunits bound to R1 sites engage the Mu termini in *trans*; domain IIβ residues of these catalytic subunits make extensive contact with the target DNA. Domain II of subunits at the R2 sites also contact the opposite DNA but in a slightly different manner, and interact with DNA-binding domains of the R1 subunits. The IIIα domains of the subunits at R2 are positioned to be proximal to the FD on the opposite Mu termini; domain IIIα has an apparent role in repair of the ST intermediate in the infection phase (53, 63), the significance of which is discussed in Transition from Transposition to Repair. The target DNA is bent through a total of ~140°, a feature also seen in the PFV intasome (21). It is hypothesized that target bending may help render ST irreversible by straining the DNA conformation such that the ends snap away from the active site after ST (62), as seen in the PVF intasome (21).

ENHANCER AND TRANSPOSOSOME TOPOLOGY

Mu is unique among transposable elements in employing an enhancer (Fig. 3A). The E DNA segment is so named because it enhances transposition over 100-fold *in vivo* and is essential for the assembly of the transpososome on native supercoiled Mu donor substrates *in vitro* (9). All the end-binding sites (L1–L3 and R1–R3) participate in interactions with E (64, 65); MuA subunits bound to these L and R sites through their Iβγ domain are expected to make cross-bridging interactions with E through their Iα domain to form the three-segment LER complex (Fig. 6). HU, which binds in the spacer region between L1 and L2 and bends the DNA, and integration host factor (IHF), which binds E and also bends DNA, both play important roles in LER interactions (Fig. 3A) (9). Although the position of the enhancer can be varied, its orientation cannot, nor can it function when present outside the Mu ends on the same DNA molecule (9); however, it can function in *trans* when supplied in 50-fold molar excess (66), from where it maintains its topological specificity and crisscrossed R1–O1 and L1–O2 interactions (67).

The path of DNA through the LER complex was mapped using a methodology called "difference topology," where the topologically well-characterized site-specific recombinase Cre was used to seal the DNA crossings within the Mu synapse (68). Using a variety of approaches, including directed positioning of MuA subunits missing the E-binding Iα domain at individual end-binding sites, the following sequence of events and topology of LER interactions was deduced: an initial ER synapse (HU-independent) captures L (HU-dependent) to form an LER complex that has five supercoils trapped within it (Fig. 6A) (69, 70). The primacy of ER interactions has been confirmed using a gel electrophoresis assay, which shows, in addition, that at the L end the L1 site is the last to join the complex (47). Of the five DNA crossings held within the Mu synapse, two are between R and E, one between L and E, and two between L and R (Fig. 6B). The E–L crossing is thought to be trapped fortuitously, while the E–R crossings are specific; except for the E–L crossing, MuA can recreate the other four DNA crossings even on nicked circular DNA in the presence of Me_2SO (71). At the R end, R1–E interaction is essential for the initial steps in the assembly, R2–E interaction is not required, and R3–E interaction contributes to the native topology (72). The data on L2–E and L3–E interactions are not unequivocal. If these interactions do occur, either one is sufficient to support the assembly process. When stripped of the loosely bound subunits, the tetrameric MuA complex retains the two L–R crossings as well as the proximal E–R crossing (Fig. 6B, black dots with white circles), but loses the E–L and distal E–R crossings; the latter crossing is formed by the MuA subunit bound at R3 (Fig. 6B,

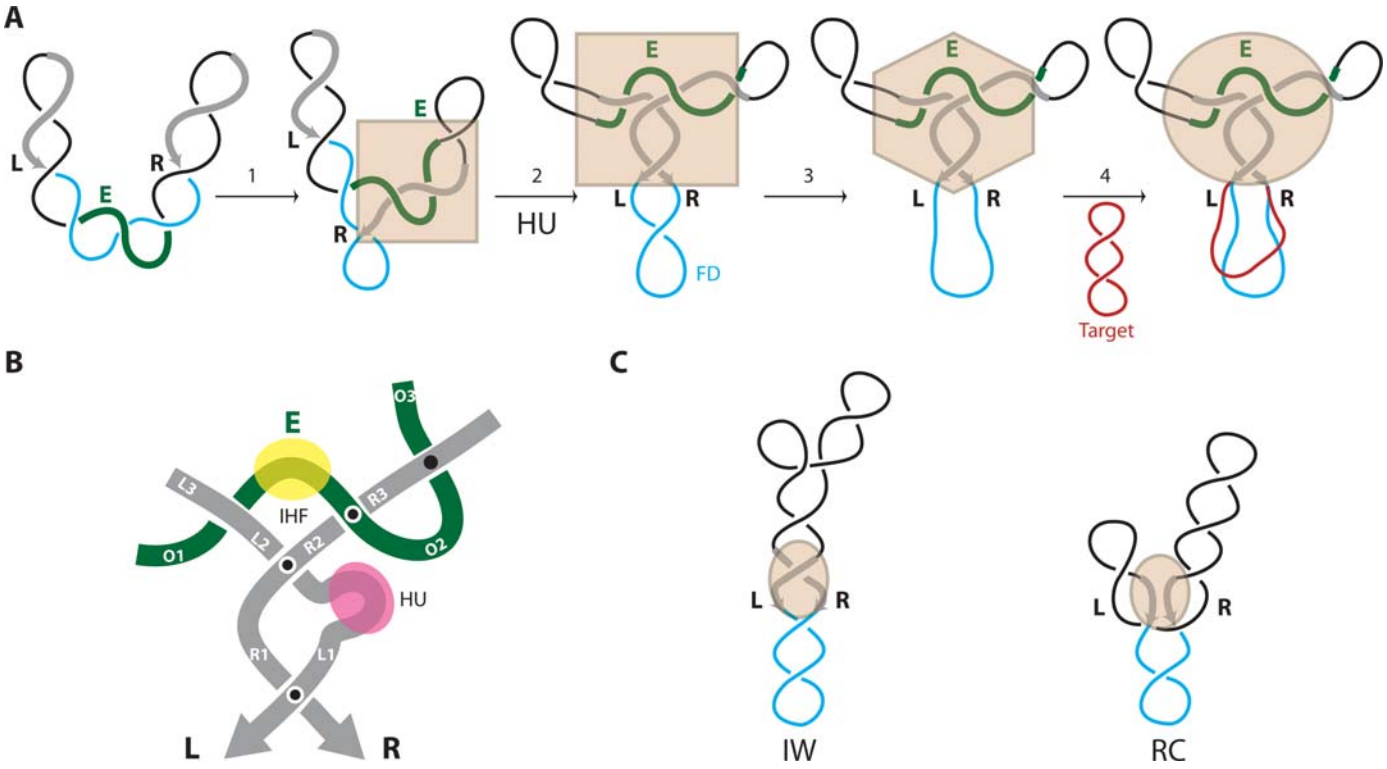

FIGURE 6 Interaction of MuA binding sites during transpososome assembly, and topology of the Mu DNA synapse. **(A)** 1. On a supercoiled DNA containing the native arrangement of L, E, and R segments, MuA-mediated interactions between E and R (square) trap two supercoil nodes within an initial ER synapse. 2. L is recruited into the ER complex with assistance from HU, and contributes one more crossing with E. The two L–R crossings within LER are fluid. 3. LER transitions into a stable complex (hexagon) which traps five supercoil nodes: two between E and R, one between E and L, and two between L and R. In this stable complex, the DNA around the Mu termini is first melted and then cleaved (see Fig. 4B, C). 4. The five-noded LER topology is maintained in the ST complex (oval), which is the most stable. **(B)** Contribution of the individual MuA-binding sites to the DNA topology. R–E interactions, particularly R1–O1, are essential in the initial stages of assembly, R2–E interactions are not required, and R3-E interactions contribute to the distal E–R crossing (black dot). Six MuA subunits (not shown) hold the five DNA crossings. The MuA tetramer retains two L–R and the proximal E–R DNA crossings (black dots with white circles). Of the two L–R crossings, the one between L1 and R1 is likely the one seen in the crystal structure (Fig. 5B). Placement of the second L–R crossing is arbitrary; see reference 72 for details. IHF binding and bending at E between O1 and O2 optimizes E interactions with L and R. HU binding and bending L between L1 and L2 delivers L1 to the ER complex (47). **(C)** Encounter and synapsis of Mu ends on supercoiled DNA. In the absence of E, the L and R ends can approach each other either by slithering to form a plectonemically interwrapped (IW) synapse or by random collision to form a random collision (RC) synapse; the presence of E channels synapsis toward the IW pathway (77). See text for details. doi:10.1128/microbiolspec.MDNA3-0007-2014.f6

black dot) (71, 72). The structure of the tetrameric Mu transpososome assembled without E and without the native arrangement of the L and R end sites shows only one L–R crossing (Fig. 5B) (62). A mathematical tangle analysis of the difference topology experiments concluded that the experimentally observed three-branched, five-crossing topological architecture of the Mu transpososome is the simplest solution, and thus biologically most likely (73, 74).

Footprinting experiments show that the Mu termini are not stably engaged in the active sites in the LER complex (Fig. 6A; see also Fig. 4A) (47). This was also

deduced from the behavior of mutant termini, which stall at the LER stage as described in the section above. These experiments show, in addition, that the enhancer changes from an apparently strained to a less strained configuration as the LER transitions from an unstable to a stable state, and that HU-promoted engagement of the L1 site with ER is the last event that triggers transition into the stable form (Fig. 6A) (47); interestingly, in a complex assembled without L1, precleaved L1 can functionally join the complex when provided in *trans*. Although E is not required for reaction chemistry (9), it remains engaged with L and R ends even after ST is completed (Fig. 6A) (47, 70), suggesting that it may play an additional role post-ST. In the minimal reaction system with R1–R2 oligonucleotide substrates, E did not enhance LR pairing, but accelerated transition to a stable form of the complex (75).

Enhancers in other site-specific recombination systems, such as the Tn3/γδ resolvase or Hin/Gin invertases, are highly selective with respect to orientation of the interacting sites and recombine through a very specific synapse topology (68). Enhancer-independent recombinases in these systems have lost the requirement for DNA supercoiling or for a specific orientation of the recombining sites. For Mu, two different enhancer-independent situations have been described. One involves an enhancer-independent transposase that, unlike the invertase and resolvase systems, does not relieve the dependence on DNA supercoiling or on the correct orientation of Mu ends (67). The other involves the addition of Me_2SO to the reaction, which does provide independence from constraints of substrate topology or site orientation (76). To determine the contribution of E to the interwrapping of Mu ends, the topology of the LR synapse was examined under the two enhancer-independent reaction conditions (77). Under the Me_2SO conditions, two topologically distinct arrangements of the ends were observed. In their normal relative orientation, L and R were either plectonemically interwrapped (IW) or aligned by random collision (RC) (Fig. 6C). Addition of the enhancer to this system channeled synapsis toward the IW pathway, showing that the enhancer imposes topological specificity on the synapse. When the ends were in the wrong relative orientation, synapsis occurred exclusively by the RC mode. In the second enhancer-independent condition, which retains the requirement for a specific orientation of Mu ends, synapsis of L and R was entirely via the IW synapse. This finding implies that the enhancer is not the only determinant of topological selectivity; the interaction of MuA with the Mu ends is also important. The mutant transposase has acquired independence from the enhancer but not from the orientation specificity of the ends. Thus, studies with this enhancer-independent Mu transposase have revealed that systems involving two-site interactions, and not necessarily three-site interactions, can also be subject to strict topological restrictions. Me_2SO conditions promote not only enhancer-independence, but independence from end orientation as well. If transposition can be supported by enhancer-independent pairing of the L and R ends, why does Mu use an enhancer? (For a discussion of this question, see reference 68.)

CENTRAL SGS SITE AND MU END PAIRING

Mu ends on plasmid substrates have no difficulty pairing, but those on a Mu prophage genome require a centrally located strong gyrase binding site (SGS) for efficient synapsis and Mu replication (78, 79). DNA gyrase bound at this site is proposed to promote the formation of a plectonemically interwound, supercoiled loop, with the site at the apex and the synapsed prophage ends at the base of the loop (Fig. 7A) (80, 81). Gyrase is known to protect and cleave within a ~100-bp region; if the cleaved region is defined as the "core" and the flanking sequences the "arms," then sequences in the right arm were delineated as an important feature of the SGS for Mu replication (82). It is speculated that the right arm may make favorable gyrase contacts, likely forming the T segment that is passed through the cleaved G segment during the supercoiling reaction. On plasmid substrates, SGS promotes highly processive supercoiling (81); this property of the Mu SGS has been exploited in studying gyrase structural dynamics using a single-molecule assay (83). Candidate SGS sequences obtained from five Mu-like prophages in different bacteria were not as proficient in supporting Mu replication, although some of them did support processive supercoiling on plasmid substrates (84).

The SGS site was seen to be important in maintaining the Mu prophage as a separate and stable chromosomal domain of *E. coli* (85). In the prophage, the two Mu ends are paired, segregating Mu into an independent chromosomal domain (Fig. 7B). The Mu domain configuration is assisted by MuB and several nucleoid-associated proteins (NAPs), and promotes low-level transcription from an early prophage promoter, which controls the expression of Mu *A* and *B*, as well as several genes not essential for phage growth, including a ligase and a Ku-like DNA repair function (86, 87). MuB might provide a NAP-like function (88). It is proposed that the Mu domain provides long-term survival benefits to both the

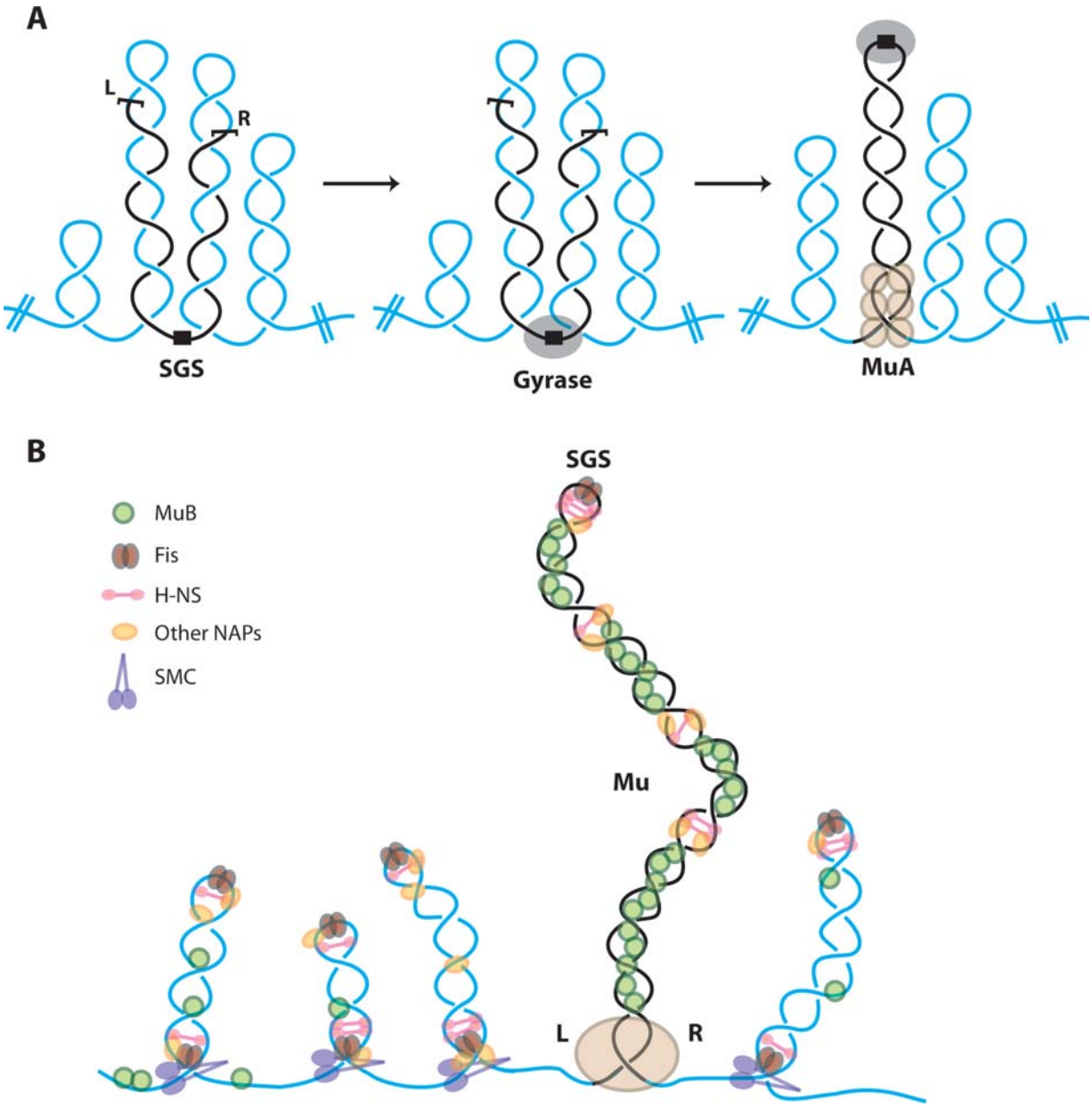

Q2

FIGURE 7 The central SGS site helps Mu prophage ends pair. **(A)** Plectonemically supercoiled domains of the *E. coli* nucleoid are shown carrying a copy of the Mu genome; L and R ends and the centrally located SGS are indicated. DNA gyrase binds at the SGS and initiates processive introduction of supercoils, leading to the extrusion of a novel nucleoid domain comprising the Mu genome in its entirety, aligning the L and R ends to promote transpososome (MuA) assembly. **(B)** A model for the structure of a Mu prophage and for Mu genome immunity. The model proposes that segregation of Mu into a separate domain, as shown in (A), is sealed by either the Mu transpososome assembled on the ends, or by nucleoid associated proteins (NAPs). Several NAPs are shown stabilizing this structure, hypothesized to promote the formation of MuB filaments. MuB, which itself has NAP-like properties, is proposed to provide immunity to self-integration. Fis and H-NS proteins may be expected to reside at the SGS and Mu ends because these proteins prefer A/T-rich regions. Sister chromatid cohesions have been proposed to be involved in the creation of large topological loops by bridging two DNAs at the base of the stem of such loops. (A) Adapted from reference 81, and reprinted with permission from John Wiley and Sons. (B) Taken from references 85 and 106. doi:10.1128/microbiolspec.MDNA3-0007-2014.f7

prophage and the host: to the prophage in bestowing transposition-ready topological properties unique to the Mu reaction and to the host in contributing extraneous DNA housekeeping functions (85).

TARGET SITE SELECTION

Mu is the most promiscuous of known mobile elements. A consensus 5-bp target recognition site 5′-NY(G/C)RN-3′ reported in early experiments (89) was refined more recently as 5′-C-Py-(G/C)-Pu-G-3′ (90); this preference is MuA encoded, and is independent of the target capture protein MuB. *In vivo*, a preference for CGG as the central triplet was observed (91). In the transpososome crystal structure, MuA is seen to contact the target DNA over a 20 to 25-bp region (Fig. 5B) (62). Analysis of target sequences *in vitro* detected symmetrical base patterns spanning a ~23 to 24-bp region around the target pentamer, indicative not of a sequence preference, but possibly of a structural preference that might facilitate target deformation (90).

Mu does not generally display an orientation bias in target selection (91), although an exception was seen at the *E. coli bgl* locus *in vivo* (92). A DNA microarray analysis of target site selection during the Mu lytic phase in both *E. coli* and *Salmonella* found hot and cold spots throughout the genome, reflecting a >1,000-fold variation in target preference (93, 94). Transcription had a strong negative influence on transposition (93), although a direct relationship between transcription and transposition is unlikely (88).

MuB is essential for target capture *in vitro* (9). A whole-genome *E. coli* tiling array revealed that there were hot and cold MuB binding sites in the genome, and that Mu transposition was in the vicinity rather than within MuB-bound regions (88). MuB is an AAA+ ATPase and a nonspecific DNA-binding protein (Fig. 3C) (34), which hydrolyzes ATP for target selection; both activities are stimulated by MuA (9). MuB forms ATP-dependent helical filaments, with or without DNA (34, 95), and has been reported to exhibit a tendency to form larger filaments on A/T-rich DNA (95, 96). Single-particle EM imaging of MuB assembled on DNA found that MuB–ATP forms a solenoid-like filament, with DNA bound in the axial channel (34). The helical parameters of the MuB filament do not match those of the B-form DNA. Despite this mismatched symmetry between the protein and DNA, MuB does not deform bound DNA (34). Based on these and other findings, it is proposed that the MuB-imposed symmetry transiently deforms DNA at the boundary of the MuB filament and results in a bent DNA conformation favored by MuA for transposition (Fig. 8A) (34). Consistent with this model, Mu transposition was observed at the junction of A/T and non-A/T DNA *in vitro* (97) and in the vicinity rather than within MuB-bound regions *in vivo* (88). Two hot spots for Mu insertion near the *bgl* locus were also observed to be clustered at the borders of an A/T-rich segment (92). Interestingly, the majority of A/T-rich regions are unavailable for MuB binding *in vivo* because they are occupied by nucleoid proteins such as Fis, which have a similar binding preference (88, 97). Other strongly DNA-bound proteins also occlude Mu insertions (94).

MuB binds DNA nonspecifically (9). Transposition in the vicinity of a specific site was achieved by fusing MuB to the site-specific DNA-binding protein Arc repressor (98). The fusion variant could select target DNA independently of ATP hydrolysis, although ADP binding was required for the MuA-stimulating activity of MuB. Thus, the ATP-binding and MuA-regulated DNA-binding activity of MuB is not essential for target delivery, but activation of MuA by MuB requires nucleotide-bound MuB. Taken together, these results suggest that target delivery by MuB occurs as a consequence of the ability of nucleotide-bound MuB to stimulate MuA while simultaneously anchoring MuA to a selected target DNA. ATP hydrolysis has a different function, as discussed below.

TRANSPOSITION IMMUNITY

cis immunity

Several bacterial transposons, including members of the Tn3 family, Tn7, and bacteriophage Mu, display transposition immunity (99, 100). These elements avoid insertion into DNA molecules that already contain a copy of the transposon (a phenomenon called *cis* immunity), and it is thought that this form of self-recognition must also provide protection against self-integration. *cis* immunity does not provide protection to the whole bacterial genome on which the transposon is resident, but can extend over large distances from the chromosomal site where the transposon is located or over an entire plasmid harboring the transposon.

In vitro studies with phage Mu provided the first molecular insights into the *cis*-immunity phenomenon (9). Using innovating fluorescence and microfluidic technology, single-molecule experiments show that MuA–MuB interaction, which stimulates the ATPase activity of MuB and promotes its dissociation from DNA, is the basis of the observed transposition immunity of mini-Mu plasmids *in vitro*; that is, MuB bound to DNA

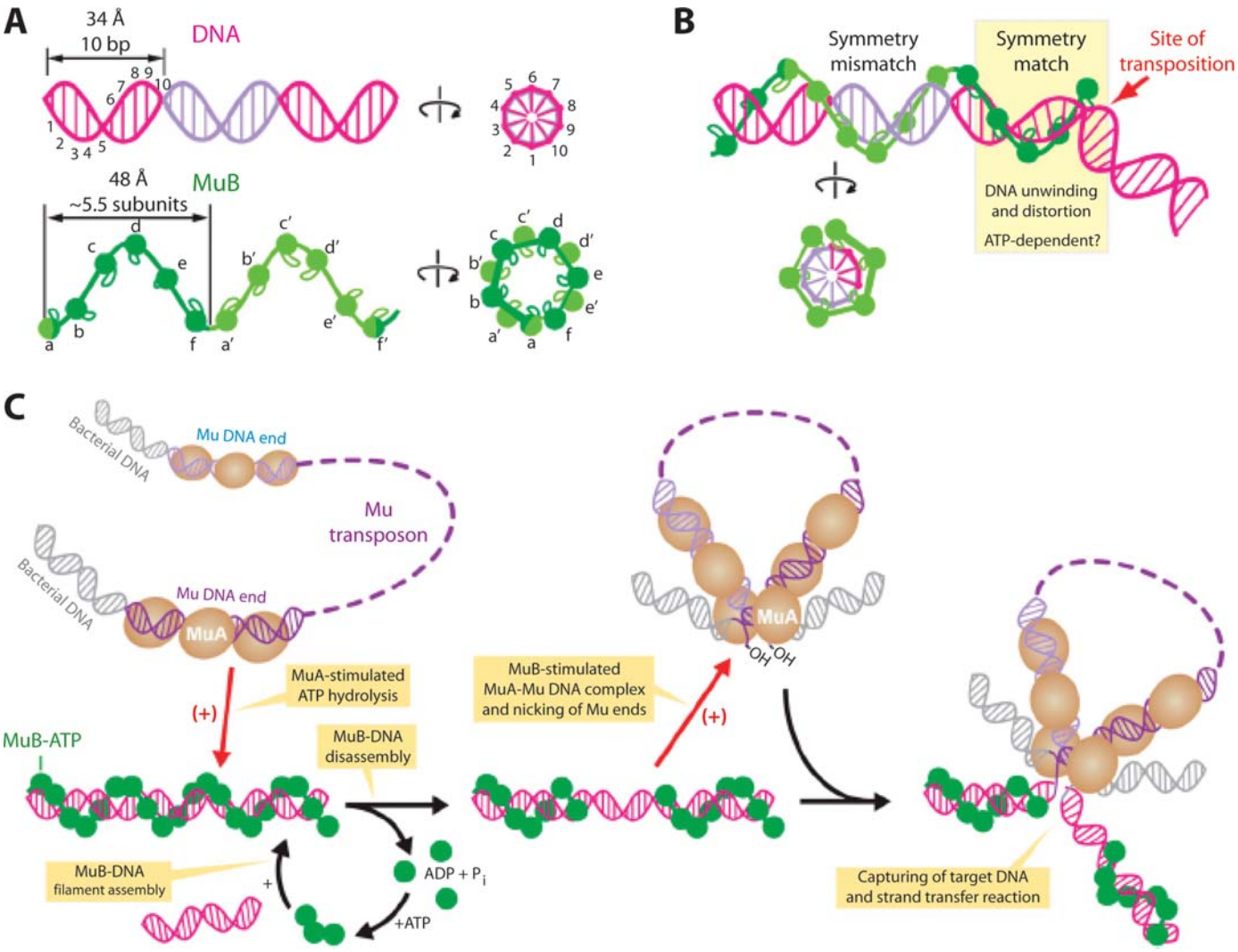

Q3

FIGURE 8 Model for MuB function in target capture and *cis* immunity. **(A)** The helical parameters of the MuB filament (represented as beads on a string) do not match those of B-form DNA. This results in a nucleoprotein complex with a symmetry mismatch. **(B)** Matching symmetry between MuB and DNA would require the DNA to be underwound and extended, which may occur at the boundary of the MuB filament with the help of MuA and possibly ATP hydrolysis. Deformed and bent DNA is a preferred target for transposition catalyzed by MuA. **(C)** A summary of interplay among MuA, MuB, and DNA during transposition. Upon ATP binding, MuB forms helical filaments on DNA. MuA bound to Mu DNA ends stimulates ATP hydrolysis by MuB and MuB dissociation from DNA, which generates MuB-free DNA regions. Reciprocally, MuB stimulates MuA to pair and nick Mu DNA ends at the junction with the flanking sequences. MuA and MuB together may induce the matching symmetry between MuB and DNA at the boundary of a MuB filament and thus DNA distortion, which leads to the target DNA capture and Mu transposition. Taken from reference 34, reprinted with permission from the *Proceedings of the National Academy of Sciences U S A*. doi:10.1128/microbiolspec.MDNA3-0007-2014.f8

dissociates upon interaction in *cis* with MuA bound to the Mu ends, resulting in MuB-free DNA, which is a poor target for new insertions (see Fig. 8B). The MuA–MuB interaction requires the formation of DNA loops between the MuA- and the MuB-bound DNA sites. Iterative loop formation/disruption cycles with intervening diffusional steps result in larger DNA loops, leading to preferential insertion of the transposon at sites

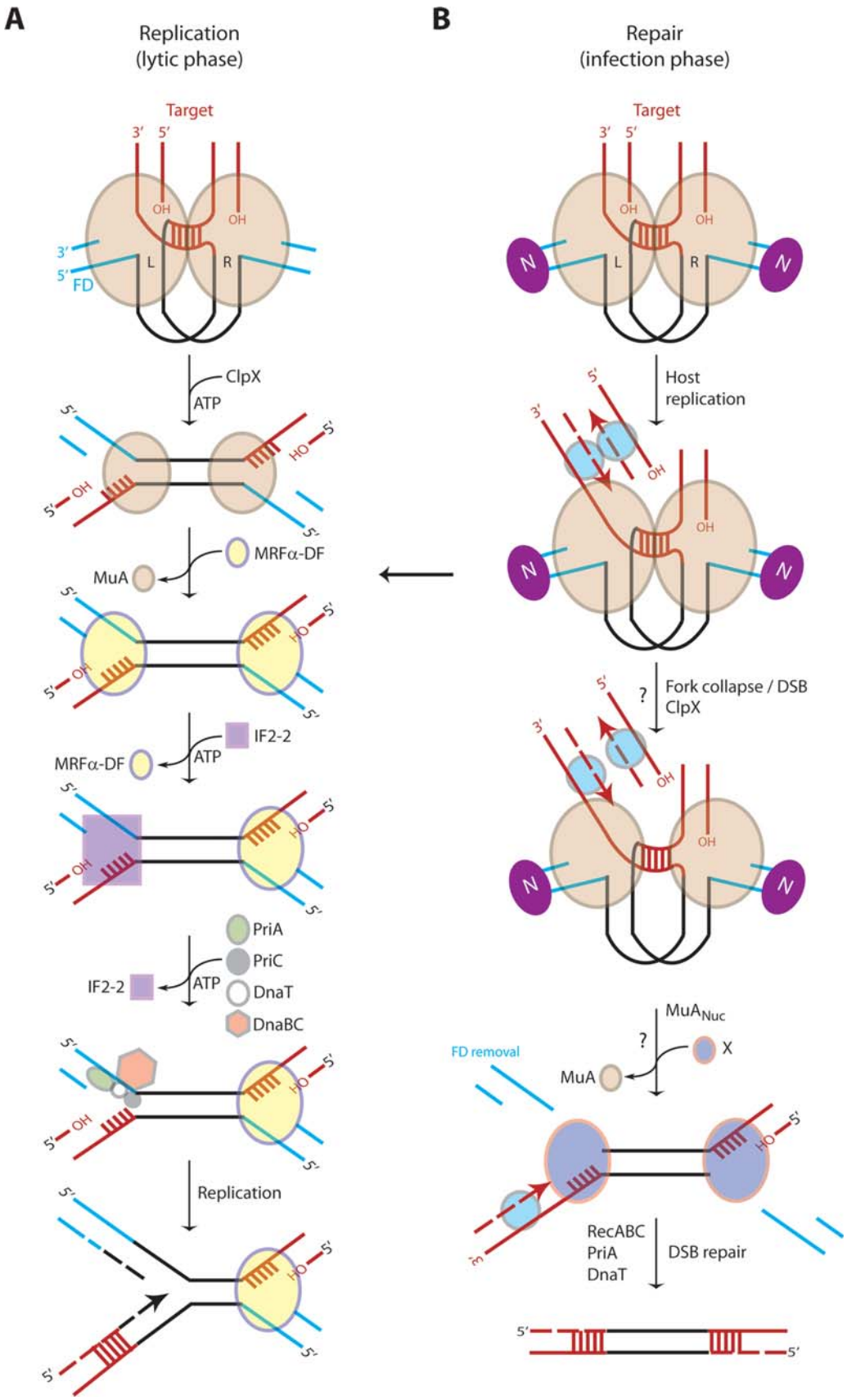
A
Replication
(lytic phase)
Target
3′ 5′
OH
OH
3′
5′
FD
L
R
ClpX
ATP
HO
5′
OH
MuA
MRFα-DF
IF2-2
ATP
PriA
PriC
DnaT
DnaBC
Replication
B
Repair
(infection phase)
N
Host
replication
?
Fork collapse / DSB
ClpX
MuA_Nuc
X
FD removal
RecABC
PriA
DnaT
DSB repair

distant from the transposon ends (101). MuB also dissociates upon interaction with MuA in *trans*, but the oligomeric state of MuA monomer, for example, when bound to ends versus multimer when assembled into an active transpososome, may distinguish interactions at the ends that underlie *cis* immunity from those that promote target capture and transposition in *trans* (Fig. 8B) (102, 103, 104). Support for a *cis*-immunity mechanism *in vivo*, which would remove MuB from the vicinity of the Mu genome, comes from studies using a 10-kb derivative of Mu (Mud), which was monitored for transposition into Tn10 elements placed at various distances from the Mud element on the *Salmonella typhimurium* chromosome (105). A gradient of insertion immunity was observed in both directions from the Mud insertion point; immunity was strongest around 5 kb outside the Mu ends.

Mu genome immunity

During the lytic phase, Mu amplifies its genome at least 100-fold. To produce viable progeny, Mu must avoid transposing into itself, a daunting task given that nearly half the host genome is composed of Mu sequences by the end of the lytic cycle and that Mu lacks target specificity. The *cis*-immunity mechanism, which is strongest around 5 kb outside the Mu ends, would not be expected to protect the 37-kb genome effectively. Indeed, the level of protection offered by this mechanism is insufficient to explain the protection seen inside Mu (106). A new immunity mechanism labeled "Mu genome immunity" has been described, which protects actively replicating Mu from self-integration (106). Unlike the *cis*-immunity mechanism, which requires removal of MuB from DNA adjacent to Mu ends, the genome-immunity mechanism is associated with strong MuB binding within the Mu genome. Sharply different patterns of MuB binding were observed inside and outside Mu, suggesting that the Mu genome is segregated into an independent chromosomal domain (Fig. 7). It is not clear why MuB would bind strongly within the Mu genome, which is not A/T rich, albeit A/T content was shown to be an unreliable predictor of MuB binding *in vivo*; MuB binding is expected to be modulated by host proteins *in vivo* (88, 97). A model for how the formation of an independent "Mu domain" might nucleate polymerization of MuB on the genome, forming a barrier against self-integration, has been proposed (Fig. 7B) (106). Mu-genome immunity might be functionally similar to the immunity conferred by the eukaryotic cellular barrier-to-autointegration factor (BAF) protein to HIV or murine leukemia virus retroviral genomes; BAF appears to play a dual role, compacting DNA reversibly to prevent autointegration on the one hand, while promoting intermolecular target capture on the other (see references in reference 106).

TRANSITION FROM TRANSPOSITION TO REPLICATION

As diagrammed in Fig. 1, the ST intermediate is resolved by replication through Mu during the lytic phase of Mu growth (107). To do so, the transpososome actively recruits the host restart replication machinery to a forked end generated by ST (Fig. 9A). In a highly choreographed series of events, the stable ST transpososome is first destabilized by the molecular chaperone ClpX, a member of the Clp/Hsp100 family of ATPases known to remodel and degrade multicomponent complexes (108). On transpososomes assembled *in vitro*, the chaperone activity of ClpX selectively unfolds one or the other of the catalytic subunits so as to destabilize (but not destroy) the entire complex (Fig. 9A) (109, 110, 111). Interestingly, MuA residues exposed only in the MuA tetramer are important for enhanced recognition by ClpX, ensuring that the tetrameric complex is a high-priority substrate (111, 112).

The ClpX-destabilized transpososome is disassembled by an as-yet unidentified host factor (Mu replication factor [MRFα-DF]), which displaces the transpososome in an ATP-independent reaction, exchanging it for a truncated form of the translation initiation factor IF2 (IF2-2) (Fig. 9A) (113). The replication restart proteins (primosome) PriA, PriC, DnaT, and the DnaB–DnaC complex then promote the binding of the replicative helicase DnaB on the lagging strand template of the

FIGURE 9 Transition from transposition to replication or repair. The ST intermediate in the lytic versus infection phase differs primarily in the configuration of the FD (see Fig. 1). **(A)** The depicted order of events was established from *in vitro* experiments (107, 113). Mu replication is known to be unidirectional, primarily initiating at the L end (8). **(B)** Repair events are deduced from *in vivo* experiments (63, 120). Question marks signify that the order of these events is not as yet established. The arrow from B to A indicates that infecting Mu can proceed directly to replication without FD removal, as seen in a domain III MuA mutant defective in FD removal (63). See text for details of both pathways.
doi:10.1128/microbiolspec.MDNA3-0007-2014.f9

Mu fork. The PriA helicase activity is needed to displace IF2-2 and plays an important role in opening the DNA duplex for DnaB binding, which promotes assembly of DNA polymerase III holoenzyme to form the restart replisome (114).

TRANSITION FROM TRANSPOSITION TO REPAIR

The ST intermediate generated during the infection phase is repaired instead of being fully replicated, as diagrammed in Fig. 1 (115). This integration event is also called nonreplicative transposition because of limited replication at the Mu ends (116). The alternate fates of a similar ST intermediate in the lytic versus the infection phase could be due to different configurations of their FD (Fig. 1). Other differences during these two phases are the differential requirements for MuB and for the host gyrase. Although both MuA and MuB are required for efficient transposition, several MuB mutants that do not support lytic transposition are proficient for the integration of infecting Mu (117, 118). *In vitro*, these mutants retain the ability to stimulate MuA, but are defective in binding and delivery of target DNA to the transpososome. These data are puzzling because transposition during the infection phase also requires target capture. The requirement for the supercoiling enzyme DNA gyrase (Fig. 7A), essential during the lytic phase, is dispensable during the infection phase (119). These data are also puzzling, given the multiple roles of supercoiling in promoting binding of MuA and HU to Mu ends (9), in arranging a special topology of the interacting sites (Fig. 6), and in the essential role of supercoiling for DNA strand separation at the Mu termini (Fig. 4).

The transition from transposition to repair (Fig. 9B) appears to be as complex as the handoff of the transpososome to the replication restart machinery (Fig. 9A). There are two repair events associated with integration during the infection phase: filling the 5-bp target gaps and removing the N-linked FD. The first is likely done by the *E. coli* replisome (Pol III) because stable Mu insertions are not recovered in the absence of the machinery responsible for double-strand break (DSB) repair—RecA, RecB, RecC, PriA, and DnaT (120); arrival of the replisome at the gap would be expected to convert the gap into a DSB (Fig. 9B). Contrary to widely held assumptions that gaps left in the target after transposition are repaired by gap-filling polymerases, PolA (Pol I) appears to not be involved in filling the Mu gaps (120). Gap-filling repair is likely coordinated with the second repair event which removes FD, but the details are not known. FD removal has been monitored by a PCR assay *in vivo* (115, 121). In the absence of ClpX, FD removal is delayed (63), suggesting that the requirement for ClpX is shared in the two pathways (Fig. 9B). MuA domain III residues, important for the cryptic nuclease activity MuA_{Nuc} (122) (Fig. 3B), are also required for FD removal (63). The requirement for ClpX and MuA_{Nuc} could be linked, in that ClpX might unmask the nuclease potential of domain III. However, such a mechanism must be suppressed in the lytic phase because removal of FD in this phase would affect the integrity of the entire chromosome (Fig. 1). Interestingly, domain III mutants that block FD removal allow replicative transposition (63), suggesting that there is a window of opportunity for FD removal, after which Mu replication can proceed by the restart pathway (Fig. 9, arrow from B to A).

MU-LIKE PHAGES

After the discovery of Mu by Larry Taylor (2), one other Mu-like phage called D108 was isolated from *E. coli* in the 1970s (123). Mu and D108 are fairly identical, except for their enhancer/operator sequences, and their respective binding regions in MuA and in the lysogenic repressor Rep. These differences have proved useful in understanding the contribution of E to transposition (65, 67, 124, 125). In the 1980s, several Mu-like phages were isolated from *Pseudomonas aeruginosa*; one of these, D3112, has been studied for its transposition properties in some detail (see reference 123). In the era of genomics, Mu-like prophages have been found in multiple distantly related species, indicating that they are widespread mobile genetic elements (126, 127). Of the mosaic Mu-like phages isolated from *P. aeruginosa* (128), *Rhodobacter capsulatus* (Rcap Mu) (129), and *Haemophilus parasuis* (130), the one from *Rhodobacter* (Rcap Mu) is similar to Mu in packaging host FD in phage particles, indicative of replicative transposition with little target site specificity. Many prophage sequences detected in Gram-negative bacteria have mosaic gene patterns, with only some Mu-like modules. Although the SGS sequences of some of these elements could substitute for the Mu SGS to varying degrees (see Central SGS Site and Mu End Pairing above) and the transposase gene from Hin-Mu in *H. influenzae* Rd was functional, as detected by *in vitro* reactions (131), there is no evidence that the majority of these more recently identified prophages are capable of active transposition. Complete and partial Mu-like prophages have been detected in several *Firmicutes* (132), opening the door for Mu-like genetic tools in Gram-positive bacteria.

MU AS A TOOL FOR GENE MANIPULATION

Since the mid-1980s, mini-Mu derivatives have been used extensively *in vivo* for insertional mutagenesis, for gene fusion and mapping, as well as for gene cloning and DNA sequencing strategies, including metabolic engineering (see references 9 and 133). More recently, the Mu enhancer element has been either supplied in *trans* or excised from mini-Mu vectors to control their transposition efficiency (reviewed in reference 133). Electroporation of *in vitro* assembled and cleaved Mu R1–R2 transpososomes has been used successfully for Mu integration in a variety of bacterial species, both Gram-positive and Gram-negative (134, 135), as well as in yeast and in mammalian genomes (136). Strong biases were seen in the target site distributions of the Mu insertion vectors in eukaryotic genomes, consistent with biases seen with other insertion vectors, illustrating the utility of Mu transpososome technology for gene transfer in eukaryotic cells. This technique has also been used to map integration sites directly using DNA barcoding and pyrosequencing (137). While MuA and MuB have been expressed in mammalian cells, integration of a transfected mini-Mu donor vector was from illegitimate recombination rather than from transposition, suggesting that Mu target capture complexes might promote nonhomologous recombination (138).

The superior target for Mu insertion presented by single nucleotide mismatches can be exploited to map genetic polymorphisms (55), as was demonstrated *in vitro* for a butterfly genome (139). Single nucleotide polymorphisms are an important resource for mapping human disease genes and have other biological applications as well (139).

SUMMARY

Transposable phage Mu has played a major role in elucidating the mechanism of movement of mobile DNA elements. The high efficiency of Mu transposition has facilitated a detailed biochemical dissection of the reaction mechanism, as well as of protein and DNA elements that regulate transpososome assembly and function. The deduced phosphotransfer mechanism involves in-line orientation of metal ion-activated hydroxyl groups for nucleophilic attack on reactive diester bonds, a mechanism that appears to be used by all transposable elements examined to date. A crystal structure of the Mu transpososome is available. Mu differs from all other transposable elements in encoding unique adaptations that promote its viral lifestyle. These adaptations include multiple DNA (enhancer, SGS) and protein (MuB, HU, IHF) elements that enable efficient Mu end synapsis, efficient target capture, low target specificity, immunity to transposition near or into itself, and efficient mechanisms for recruiting host repair and replication machineries to resolve transposition intermediates. MuB has multiple functions, including target capture and immunity. The SGS element promotes gyrase-mediated Mu end synapsis and the enhancer, aided by HU and IHF, participate in directing a unique topological architecture of the Mu synapse. The function of these DNA and protein elements is important during both lysogenic and lytic phases. Enhancer properties have been exploited in the design of mini-Mu vectors for genetic engineering. Mu ends assembled into active transpososomes have been delivered directly into bacterial, yeast and human genomes, where they integrate efficiently, and may prove useful for gene therapy.

ACKNOWLEDGMENTS

The principal support for Mu research in my lab has come from a long-running grant from the National Institutes of Health, and partial support by the Robert Welch foundation. I am grateful to Rudra Saha for assistance with the illustrations in this article.

REFERENCES

1. Harshey RM. 2012. The Mu story: how a maverick phage moved the field forward. *Mob DNA* **3:**21.

2. Taylor AL. 1963. Bacteriophage-induced mutations in *E. coli*. *Proc Natl Acad Sci USA* **50:**1043–1051.

3. McClintock B. 1950. The origin and behavior of mutable loci in maize. *Proc Natl Acad Sci USA* **36:**344–355.

4. Ljungquist E, Bukhari AI. 1977. State of prophage Mu DNA upon induction. *Proc Natl Acad Sci USA* **74:**3143–3147.

5. Faelen M, Huisman O, Toussaint A. 1978. Involvement of phage Mu-1 early functions in Mu-mediated chromosomal rearrangements. *Nature* **271:**580–582.

6. Shapiro JA. 1979. Molecular model for the transposition and replication of bacteriophage Mu and other transposable elements. *Proc Natl Acad Sci USA* **76:**1933–1937.

7. Mizuuchi K. 1983. *In vitro* transposition of bacteriophage Mu: a biochemical approach to a novel replication reaction. *Cell* **35:**785–794.

8. Symonds N, Toussaint A, Van de Putte P, Howe MM. 1987. *Phage Mu*. Cold Spring Harbor Laboratory, Cold Spring Harbor, NY.

9. Chaconas G, Harshey RM. 2002. Transposition of phage Mu DNA, p 384–402. *In* Craig NL, Craigie R, Gellert M, Lambowitz AM (ed), *Mobile DNA II*. ASM Press, Washington, DC.

10. Mizuuchi K, Baker TA. 2002. Chemical mechanisms for mobilizing DNA, p 12–23. *In* Craig NL, Craigie R, Gellert M, Lambowitz AM (ed), *Mobile DNA II*. ASM Press, Washington, DC.

11. Harshey RM, Bukhari AI. 1983. Infecting bacteriophage Mu DNA forms a circular DNA-protein complex. *J Mol Biol* **167:**427–441.

12. Puspurs AH, Trun NJ, Reeve JN. 1983. Bacteriophage Mu DNA circularizes following infection of *Escherichia coli*. *EMBO J* **2:**345–352.

13. Gloor G, Chaconas G. 1988. Sequence of bacteriophage Mu N and P genes. *Nucleic Acids Res* **16:**5211–5212.

14. Lassila JK, Zalatan JG, Herschlag D. 2011. Biological phosphoryl-transfer reactions: understanding mechanism and catalysis. *Annu Rev Biochem* **80:**669–702.

15. Lewinski MK, Bushman FD. 2005. Retroviral DNA integration–mechanism and consequences. *Adv Genet* **55:**147–181.

16. Montano SP, Rice PA. 2011. Moving DNA around: DNA transposition and retroviral integration. *Curr Opin Struct Biol* **21:**370–378.

17. Kennedy AK, Haniford DB, Mizuuchi K. 2000. Single active site catalysis of the successive phosphoryl transfer steps by DNA transposases: insights from phosphorothioate stereoselectivity. *Cell* **101:**295–305.

18. Mizuuchi K, Adzuma K. 1991. Inversion of the phosphate chirality at the target site of Mu DNA strand transfer: evidence for a one-step transesterification mechanism. *Cell* **66:**129–140.

19. Nowotny M, Gaidamakov SA, Crouch RJ, Yang W. 2005. Crystal structures of RNase H bound to an RNA/DNA hybrid: substrate specificity and metal-dependent catalysis. *Cell* **121:**1005–1016.

20. Mizuuchi K. 1992. Polynucleotidyl transfer reactions in transpositional DNA recombination. *J Biol Chem* **267:**21273–21276.

21. Maertens GN, Hare S, Cherepanov P. 2010. The mechanism of retroviral integration from X-ray structures of its key intermediates. *Nature* **468:**326–329.

22. Hare S, Gupta SS, Valkov E, Engelman A, Cherepanov P. 2010. Retroviral intasome assembly and inhibition of DNA strand transfer. *Nature* **464:**232–236.

23. Hare S, Maertens GN, Cherepanov P. 2012. 3′-processing and strand transfer catalysed by retroviral integrase *in crystallo*. *EMBO J* **31:**3020–3028.

24. Chow SA, Vincent KA, Ellison V, Brown PO. 1992. Reversal of integration and DNA splicing mediated by integrase of human immunodeficiency virus. *Science* **255:**723–726.

25. Jonsson CB, Donzella GA, Roth MJ. 1993. Characterization of the forward and reverse integration reactions of the Moloney murine leukemia virus integrase protein purified from *Escherichia coli*. *J Biol Chem* **268:**1462–1469.

26. Polard P, Ton-Hoang B, Haren L, Betermier M, Walczak R, Chandler M. 1996. IS911-mediated transpositional recombination *in vitro*. *J Mol Biol* **264:**68–81.

27. Beall EL, Rio DC. 1998. Transposase makes critical contacts with, and is stimulated by, single-stranded DNA at the P element termini *in vitro*. *EMBO J* **17:**2122–2136.

28. Melek M, Gellert M. 2000. RAG1/2-mediated resolution of transposition intermediates: two pathways and possible consequences. *Cell* **101:**625–633.

29. Au TK, Pathania S, Harshey RM. 2004. True reversal of Mu integration. *EMBO J* **23:**3408–3420.

30. Mizuuchi M, Rice PA, Wardle SJ, Haniford DB, Mizuuchi K. 2007. Control of transposase activity within a transpososome by the configuration of the flanking DNA segment of the transposon. *Proc Natl Acad Sci USA* **104:**14622–14627.

31. Surette MG, Buch SJ, Chaconas G. 1987. Transpososomes: stable protein-DNA complexes involved in the *in vitro* transposition of bacteriophage Mu DNA. *Cell* **49:**253–262.

32. Cherepanov P, Maertens GN, Hare S. 2011. Structural insights into the retroviral DNA integration apparatus. *Curr Opin Struct Biol* **21:**249–256.

33. Lemberg KM, Schweidenback CT, Baker TA. 2007. The dynamic Mu transpososome: MuB activation prevents disintegration. *J Mol Biol* **374:**1158–1171.

34. Mizuno N, Dramicanin M, Mizuuchi M, Adam J, Wang Y, Han YW, Yang W, Steven AC, Mizuuchi K, Ramon-Maiques S. 2013. MuB is an AAA+ ATPase that forms helical filaments to control target selection for DNA transposition. *Proc Natl Acad Sci USA* **110:**E2441–2450.

35. Coros CJ, Sekino Y, Baker TA, Chaconas G. 2003. Effect of mutations in the C-terminal domain of Mu B on DNA binding and interactions with Mu A transposase. *J Biol Chem* **278:**31210–31217.

36. Williams TL, Baker TA. 2004. Reorganization of the Mu transpososome active sites during a cooperative transition between DNA cleavage and joining. *J Biol Chem* **279:**5135–5145.

37. Savilahti H, Rice PA, Mizuuchi K. 1995. The phage Mu Transpososome core—DNA requirements for assembly and function. *EMBO J* **14:**4893–4903.

38. Wang Z, Harshey RM. 1994. Crucial role for DNA supercoiling in Mu transposition: a kinetic study. *Proc Natl Acad Sci USA* **91:**699–703.

39. Wang Z, Namgoong SY, Zhang X, Harshey RM. 1996. Kinetic and structural probing of the precleavage synaptic complex (type 0) formed during phage Mu transposition. Action of metal ions and reagents specific to single-stranded DNA. *J Biol Chem* **271:**9619–9626.

40. Yanagihara K, Mizuuchi K. 2003. Progressive structural transitions within Mu transpositional complexes. Mol. *Cell* **11:**215–224.

41. Lee I, Harshey RM. 2003. Patterns of sequence conservation at termini of long terminal repeat (LTR) retrotransposons and DNA transposons in the human genome: lessons from phage Mu. *Nucleic Acids Res* **31:**4531–4540.

42. El Hassan MA, Calladine CR. 1997. Conformational characteristics of DNA: empirical classifications and a hypothesis for the conformational behaviour of dinucleotide steps. *Phil Trans R Soc Lond* **355:**43–100.

43. Lee I, Harshey RM. 2001. Importance of the conserved CA dinucleotide at Mu termini. *J Mol Biol* **314:**433–444.

44. Goldhaber-Gordon I, Early MH, Baker TA. 2003. The terminal nucleotide of the Mu genome controls catalysis of DNA strand transfer. *Proc Natl Acad Sci USA* **100:**7509–7514.

45. Watson MA, Chaconas G. 1996. Three-site synapsis during Mu DNA transposition: A critical intermediate preceding engagement of the active site. *Cell* **85:** 435–445.

46. Lee I, Harshey RM. 2003. The conserved CA/TG motif at Mu termini: T specifies stable transpososome assembly. *J Mol Biol* **330:**261–275.

47. Kobryn K, Watson MA, Allison RG, Chaconas G. 2002. The Mu three-site synapse: a strained assembly platform in which delivery of the L1 transposase binding site triggers catalytic commitment. *Mol Cell* **10:**659–669.

48. Goldhaber-Gordon I, Williams TL, Baker TA. 2002. DNA recognition sites activate MuA transposase to perform transposition of non-Mu DNA. *J Biol Chem* **277:**7694–7702.

49. Goldhaber-Gordon I, Early MH, Gray MK, Baker TA. 2002. Sequence and positional requirements for DNA sites in a mu transpososome. *J Biol Chem* **277:**7703–7712.

50. Saariaho AH, Savilahti H. 2006. Characteristics of MuA transposase-catalyzed processing of model transposon end DNA hairpin substrates. *Nucleic Acids Res* **34:**3139–3149.

51. Coros CJ, Chaconas G. 2001. Effect of mutations in the Mu-host junction region on transpososome assembly. *J Mol Biol* **310:**299–309.

52. Surette MG, Harkness T, Chaconas G. 1991. Stimulation of the Mu A protein-mediated strand cleavage reaction by the Mu B protein, and the requirement of DNA nicking for stable type 1 transpososome formation. *In vitro* transposition characteristics of mini-Mu plasmids carrying terminal base pair mutations. *J Biol Chem* **266:**3118–3124.

53. Mariconda S, Namgoong SY, Yoon KH, Jiang H, Harshey RM. 2000. Domain III function of Mu transposase analysed by directed placement of subunits within the transpososome. *J Biosci* **25:**347–360.

54. Naigamwalla DZ, Chaconas G. 1997. A new set of Mu DNA transposition intermediates: alternate pathways of target capture preceding strand transfer. *EMBO J* **16:**5227–5234.

55. Yanagihara K, Mizuuchi K. 2002. Mismatch-targeted transposition of Mu: a new strategy to map genetic polymorphism. *Proc Natl Acad Sci USA* **99:**11317–11321.

56. Craig NL, Craigie, R, Gellert, M, Lambowitz, AM. 2002. *Mobile DNA II*. ASM Press, Washington, DC.

57. Steiniger-White M, Rayment I, Reznikoff WS. 2004. Structure/function insights into Tn5 transposition. *Curr Opin Struct Biol* **14:**50–57.

58. Barabas O, Ronning DR, Guynet C, Hickman AB, Ton-Hoang B, Chandler M, & Dyda F. 2008. Mechanism of IS200/IS605 family DNA transposases: activation and transposon-directed target site selection. *Cell* **132:**208–220.

59. Richardson JM, Colloms SD, Finnegan DJ, Walkinshaw MD. 2009. Molecular architecture of the Mos1 paired-end complex: the structural basis of DNA transposition in a eukaryote. *Cell* **138:**1096–1108.

60. Grandgenett D, Korolev S. 2010. Retrovirus integrase-DNA structure elucidates concerted integration mechanisms. *Viruses* **2:**1185–1189.

61. Yuan JF, Beniac DR, Chaconas G, Ottensmeyer FP. 2005. 3D reconstruction of the Mu transposase and the Type 1 transpososome: a structural framework for Mu DNA transposition. *Genes Dev* **19:**840–852.

62. Montano SP, Pigli YZ, Rice PA. 2012. The Mu transpososome structure sheds light on DDE recombinase evolution. *Nature* **491:**413–417.

63. Choi W, Harshey RM. 2010. DNA repair by the cryptic endonuclease activity of Mu transposase. *Proc Natl Acad Sci USA* **107:**10014–10019.

64. Allison RG, Chaconas G. 1992. Role of the A protein-binding sites in the *in vitro* transposition of Mu DNA. A complex circuit of interactions involving the Mu ends and the transpositional enhancer. *J Biol Chem* **267:**19963–19970.

65. Jiang H, Yang JY, Harshey RM. 1999. Criss-crossed interactions between the enhancer and the att sites of phage Mu during DNA transposition. *EMBO J* **18:**3845–3855.

66. Surette MG, Chaconas G. 1992. The Mu transpositional enhancer can function in *trans*: requirement of the enhancer for synapsis but not strand cleavage. *Cell* **68:**1101–1108.

67. Jiang H, Harshey RM. 2001. The Mu enhancer is functionally asymmetric both in *cis* and in *trans*. Topological selectivity of Mu transposition is enhancer-independent. *J Biol Chem* **276:**4373–4381.

68. Harshey RM, Jayaram M. 2006. The Mu transpososome through a topological lens. *Crit Rev Biochem Mol Biol* **41:**387–405.

69. Pathania S, Jayaram M, Harshey RM. 2002. Path of DNA within the Mu transpososome. Transposase interactions bridging two Mu ends and the enhancer trap five DNA supercoils. *Cell* **109:**425–436.

70. Pathania S, Jayaram M, Harshey RM. 2003. A unique right end-enhancer complex precedes synapsis of Mu ends: the enhancer is sequestered within the transpososome throughout transposition. *EMBO J* **22:**3725–3736.

71. Yin Z, Jayaram M, Pathania S, Harshey RM. 2005. The Mu transposase interwraps distant DNA sites within a functional transpososome in the absence of DNA supercoiling. *J Biol Chem* **280:**6149–6156.

72. Yin Z, Suzuki A, Lou Z, Jayaram M, Harshey RM. 2007. Interactions of phage Mu enhancer and termini that specify the assembly of a topologically unique interwrapped transpososome. *J Mol Biol* **372:**382–396.

73. Darcy IK, Chang J, Druivenga N, McKinney C, Medikonduri RK, Mills S, Navarra-Madsen J, Ponnusamy A, Sweet J, Thompson T. 2006. Coloring the Mu transpososome. *BMC Bioinformatics* **7:**435.

74. Darcy IK, Luecke J, Vazquez M. 2009. Tangle analysis of difference topology experiments: applications to a Mu protein–DNA complex. *Algebr Geom Topol* **9:**2247–2309.

75. Mizuuchi M, Mizuuchi K. 2001. Conformational isomerization in phage Mu transpososome assembly: effects of the transpositional enhancer and of MuB. *EMBO J* **20:**6927–6935.

76. Mizuuchi M, Mizuuchi K. 1989. Efficient Mu transposition requires interaction of transposase with a DNA sequence at the Mu operator: implications for regulation. *Cell* **58:**399–408.

77. Yin Z, Harshey RM. 2005. Enhancer-independent Mu transposition from two topologically distinct synapses. *Proc Natl Acad Sci USA* **102:**18884–18889.

78. Pato ML, Banerjee M. 2000. Genetic analysis of the strong gyrase site (SGS) of bacteriophage Mu: localization of determinants required for promoting Mu replication. *Mol Microbiol* **37:**800–810.

79. Pato ML. 2004. Replication of Mu prophages lacking the central strong gyrase site. *Res Microbiol* **155:**553–558.

80. Pato ML, Banerjee M. 1996. The Mu strong gyrase-binding site promotes efficient synapsis of the prophage termini. *Mol Microbiol* **22:**283–292.

81. Oram M, Howells AJ, Maxwell A, Pato ML. 2003. A biochemical analysis of the interaction of DNA gyrase with the bacteriophage Mu, pSC101 and pBR322 strong gyrase sites: the role of DNA sequence in modulating gyrase supercoiling and biological activity. *Mol Microbiol* **50:**333–347.

82. Oram M, Travers AA, Howells AJ, Maxwell A, Pato ML. 2006. Dissection of the bacteriophage Mu strong gyrase site (SGS): significance of the SGS right arm in Mu biology and DNA gyrase mechanism. *J Bacteriol* **188:**619–632.

83. Basu A, Schoeffler AJ, Berger JM, Bryant Z. 2012. ATP binding controls distinct structural transitions of Escherichia coli DNA gyrase in complex with DNA. *Nat Struct Mol Biol* **19:**538–546, S531.

84. Oram M, Pato ML. 2004. Mu-like prophage strong gyrase site sequences: analysis of properties required for promoting efficient Mu DNA replication. *J Bacteriol* **186:**4575–4584.

85. Saha RP, Lou Z, Meng L, Harshey RM. 2013. Transposable prophage Mu is organized as a stable chromosomal domain of *E. coli*. *PLoS Genet* **9:**e1003902.

86. Paolozzi L, Ghelardini P. 1992. A case of lysogenic conversion: modification of cell phenotype by constitutive expression of the Mu gem operon. *Res Microbiol* **143:**237–243.

87. d'Adda di Fagagna F, Weller GR, Doherty AJ, Jackson SP. 2003. The Gam protein of bacteriophage Mu is an orthologue of eukaryotic Ku. *EMBO Rep* **4:**47–52.

88. Ge J, Lou Z, Cui H, Shang L, Harshey RM. 2011. Analysis of phage Mu DNA transposition by whole-genome *Escherichia coli* tiling arrays reveals a complex relationship to distribution of target selection protein B, transcription and chromosome architectural elements. *J Biosci* **36:**587–601.

89. Mizuuchi M, Mizuuchi K. 1993. Target site selection in transposition of phage Mu. *Cold Spring Harb Symp Quant Biol* **58:**515–523.

90. Haapa-Paananen S, Rita H, Savilahti H. 2002. DNA transposition of bacteriophage Mu. A quantitative analysis of target site selection *in vitro*. *J Biol Chem* **277:**2843–2851.

91. Manna D, Deng S, Breier AM, Higgins NP. 2005. Bacteriophage Mu targets the trinucleotide sequence CGG. *J Bacteriol* **187:**3586–3588.

92. Manna D, Wang X, Higgins NP. 2001. Mu and IS1 transpositions exhibit strong orientation bias at the *Escherichia coli bgl* locus. *J Bacteriol* **183:**3328–3335.

93. Manna D, Breier AM, Higgins NP. 2004. Microarray analysis of transposition targets in *Escherichia coli*: the impact of transcription. *Proc Natl Acad Sci USA* **101:**9780–9785.

94. Manna D, Porwollik S, McClelland M, Tan R, Higgins NP. 2007. Microarray analysis of Mu transposition in *Salmonella enterica*, serovar Typhimurium: transposon exclusion by high-density DNA binding proteins. *Mol Microbiol* **66:**315–328.

95. Greene EC, Mizuuchi K. 2004. Visualizing the assembly and disassembly mechanisms of the MuB transposition targeting complex. *J Biol Chem* **279:**16736–16743.

96. Tan X, Mizuuchi M, Mizuuchi K. 2007. DNA transposition target immunity and the determinants of the MuB distribution patterns on DNA. *Proc Natl Acad Sci USA* **104:**13925–13929.

97. Ge J, Harshey RM. 2008. Congruence of *in vivo* and *in vitro* insertion patterns in hot *E. coli* gene targets of transposable element Mu: opposing roles of MuB in target capture and integration. *J Mol Biol* **380:**598–607.

98. Schweidenback CT, Baker TA. 2008. Dissecting the roles of MuB in Mu transposition: ATP regulation of DNA binding is not essential for target delivery. *Proc Natl Acad Sci USA* **105:**12101–12107.

99. Craig NL. 1997. Target site selection in transposition. *Annu Rev Biochem* **66:**437–474.

100. Lambin M, Nicolas E, Oger CA, Nguyen N, Prozzi D, Hallet B. 2012. Separate structural and functional domains of Tn4430 transposase contribute to target immunity. *Mol Microbiol* **83:**805–820.

101. Han YW, Mizuuchi K. 2010. Phage Mu transposition immunity: protein pattern formation along DNA by a diffusion-ratchet mechanism. *Mol Cell* **39:**48–58.

102. Greene EC, Mizuuchi K. 2002. Direct observation of single MuB polymers: evidence for a DNA-dependent conformational change for generating an active target complex. *Mol Cell* **9:**1079–1089.

103. Greene EC, Mizuuchi K. 2002. Dynamics of a protein polymer: the assembly and disassembly pathways of the MuB transposition target complex. *EMBO J* **21:**1477–1486.

104. Greene EC, Mizuuchi K. 2002. Target immunity during Mu DNA transposition. Transpososome assembly and DNA looping enhance MuA-mediated disassembly of the MuB target complex. *Mol Cell* **10:**1367–1378.

105. Manna D, Higgins NP. 1999. Phage Mu transposition immunity reflects supercoil domain structure of the chromosome. *Mol Microbiol* **32:**595–606.

106. Ge J, Lou Z, Harshey RM. 2010. Immunity of replicating Mu to self-integration: a novel mechanism employing MuB protein. *Mob. DNA* **1:**8.

107. Nakai H, Doseeva V, Jones JM. 2001. Handoff from recombinase to replisome: insights from transposition. *Proc Natl Acad Sci USA* **98:**8247–8254.

108. Baker TA, Sauer RT. 2012. ClpXP, an ATP-powered unfolding and protein-degradation machine. *Biochim Biophys Acta* **1823:**15–28.

109. Burton BM, Williams TL, Baker TA. 2001. ClpX-mediated remodeling of Mu transpososomes: selective unfolding of subunits destabilizes the entire complex. *Mol Cell* **8:**449–454.

110. Burton BM, Baker TA. 2003. Mu transpososome architecture ensures that unfolding by ClpX or proteolysis by ClpXP remodels but does not destroy the complex. *Chem Biol* **10:**463–472.

111. Abdelhakim AH, Sauer RT, Baker TA. 2010. The AAA+ ClpX machine unfolds a keystone subunit to remodel the Mu transpososome. *Proc Natl Acad Sci USA* **107:**2437–2442.

112. Abdelhakim AH, Oakes EC, Sauer RT, Baker TA. 2008. Unique contacts direct high-priority recognition of the tetrameric Mu transposase-DNA complex by the AAA+ unfoldase ClpX. *Mol Cell* **30:**39–50.

113. North SH, Kirtland SE, Nakai H. 2007. Translation factor IF2 at the interface of transposition and replication by the PriA-PriC pathway. *Mol Microbiol* **66:**1566–1578.

114. North SH, Nakai H. 2005. Host factors that promote transpososome disassembly and the PriA-PriC pathway for restart primosome assembly. *Mol Microbiol* **56:**1601–1616.

115. Au TK, Agrawal P, Harshey RM. 2006. Chromosomal integration mechanism of infecting mu virion DNA. *J Bacteriol* **188:**1829–1834.

116. Harshey RM. 1984. Transposition without duplication of infecting bacteriophage Mu DNA. *Nature* **311:**580–581.

117. Chaconas G, Giddens EB, Miller JL, Gloor G. 1985. A truncated form of the bacteriophage Mu B protein promotes conservative integration, but not replicative transposition, of Mu DNA. *Cell* **41:**857–865.

118. Roldan LA, Baker TA. 2001. Differential role of the Mu B protein in phage Mu integration vs. replication: mechanistic insights into two transposition pathways. *Mol Microbiol* **40:**141–155.

119. Sokolsky TD, Baker TA. 2003. DNA gyrase requirements distinguish the alternate pathways of Mu transposition. *Mol Microbiol* **47:**397–409.

120. Jang S, Sandler SJ, Harshey RM. 2012. Mu insertions are repaired by the double-strand break repair pathway of *Escherichia coli*. *PLoS Genet* **8:**e1002642.

121. Chaconas G, Kennedy DL, Evans D. 1983. Predominant integration end products of infecting bacteriophage Mu DNA are simple insertions with no preference for integration of either Mu DNA strand. *Virology* **128:**48–59.

122. Wu Z, Chaconas G. 1995. A novel DNA binding and nuclease activity in domain III of Mu transposase: evidence for a catalytic region involved in donor cleavage. *EMBO J* **14:**3835–3843.

123. DuBow MS. 1987. Transposable Mu-like phages, pp 201–213. *In* Symonds N, Toussaint A, Putte V.D.P., Howe MM (ed), *Phage Mu*. Cold Spring Harbor Laboratory, Cold Spring Harbor, NY.

124. Yang JY, Jayaram M, Harshey RM. 1995. Enhancer-independent variants of phage Mu transposase—enhancer-specific stimulation of catalytic activity by a partner transposase. *Genes Dev* **9:**2545–2555.

125. Yang JY, Kim K, Jayaram M, Harshey RM. 1995. A domain sharing model for active site assembly within the Mu A tetramer during transposition: the enhancer may specify domain contributions. *EMBO J* **14:**2374–2384.

126. Morgan GJ, Hatfull GF, Casjens S, Hendrix RW. 2002. Bacteriophage Mu genome sequence: analysis and comparison with Mu-like prophages in *Haemophilus, Neisseria* and *Deinococcus*. *J Mol Biol* **317:**337–359.

127. Casjens S. 2003. Prophages and bacterial genomics: what have we learned so far? *Mol Microbiol* **49:**277–300.

128. Wang PW, Chu L, Guttman DS. 2004. Complete sequence and evolutionary genomic analysis of the *Pseudomonas aeruginosa* transposable bacteriophage D3112. *J Bacteriol* **186:**400–410.

129. Fogg PC, Hynes AP, Digby E, Lang AS, Beatty JT. 2011. Characterization of a newly discovered Mu-like bacteriophage, RcapMu, in *Rhodobacter capsulatus* strain SB1003. *Virology* **421:**211–221.

130. Zehr ES, Tabatabai LB, Bayles DO. 2012. Genomic and proteomic characterization of SuMu, a Mu-like bacteriophage infecting *Haemophilus parasuis*. *BMC Genomics* **13:**331.

131. Saariaho AH, Lamberg A, Elo S, Savilahti H. 2005. Functional comparison of the transposition core machineries of phage Mu and *Haemophilus influenzae* Mu-like prophage Hin-Mu reveals interchangeable components. *Virology* **331:**6–19.

132. Toussaint A. 2013. Transposable Mu-like phages in Firmicutes: new instances of divergence generating retroelements. *Res Microbiol* **164:**281–287.

133. Akhverdyan VZ, Gak ER, Tokmakova IL, Stoynova NV, Yomantas YA, Mashko SV. 2011. Application of the bacteriophage Mu-driven system for the integration/amplification of target genes in the chromosomes of engineered Gram-negative bacteria. *Appl Microbiol Biotechnol* **91:**857–871.

134. Lamberg A, Nieminen S, Qiao M, Savilahti H. 2002. Efficient insertion mutagenesis strategy for bacterial genomes involving electroporation of *in vitro*-assembled DNA transposition complexes of bacteriophage Mu. *Appl Environ Microbiol* **68:**705–712.

135. Pajunen MI, Pulliainen AT, Finne J, Savilahti H. 2005. Generation of transposon insertion mutant libraries for Gram-positive bacteria by electroporation of phage Mu DNA transposition complexes. *Microbiology* **151:**1209–1218.

136. Paatero AO, Turakainen H, Happonen LJ, Olsson C, Palomaki T, Pajunen MI, Meng X, Otonkoski T, Tuuri T, Berry C, Malani N, Frilander MJ, Bushman FD, Savilahti H. 2008. Bacteriophage Mu integration in yeast and mammalian genomes. *Nucleic Acids Res* **36:**e148.

137. Brady T, Roth SL, Malani N, Wang GP, Berry CC, Leboulch P, Hacein-Bey-Abina S, Cavazzana-Calvo M, Papapetrou EP, Sadelain M, Savilahti H, Bushman FD. 2011. A method to sequence and quantify DNA integration for monitoring outcome in gene therapy. *Nucleic Acids Res* **39:**e72.

138. Schagen FH, Rademaker HJ, Cramer SJ, van Ormondt H, van der Eb AJ, van de Putte P, & Hoeben RC. 2000. Towards integrating vectors

for gene therapy: expression of functional bacteriophage MuA and MuB proteins in mammalian cells. *Nucleic Acids Res* **28:**E104.

139. Orsini L, Pajunen M, Hanski I, Savilahti H. 2007. SNP discovery by mismatch-targeting of Mu transposition. *Nucleic Acids Res* **35:**e44.

140. Nakayama C, Teplow DB, Harshey RM. 1987. Structural domains in phage Mu transposase: identification of the site-specific DNA-binding domain. *Proc Natl Acad Sci USA* **84:**1809–1813.

141. Rice PA. 2005. Visualizing Mu transposition: assembling the puzzle pieces. *Genes Dev* **19:**773–775.

142. Rice P, Mizuuchi K. 1995. Structure of the bacteriophage Mu transposase core: a common structural motif for DNA transposition and retroviral integration. *Cell* **82:**209–220.

143. Rasila TS, Vihinen M, Paulin L, Haapa-Paananen S, Savilahti H. 2012. Flexibility in MuA transposase family protein structures: functional mapping with scanning mutagenesis and sequence alignment of protein homologues. *PLoS One* **7:**e37922.

144. Teplow DB, Nakayama C, Leung PC, Harshey RM. 1988. Structure-function relationships in the transposition protein B of bacteriophage Mu. *J Biol Chem* **263:**10851–10857.

145. Hung LH, Chaconas G, Shaw GS. 2000. The solution structure of the C-terminal domain of the Mu B transposition protein. *EMBO J* **19:**5625–5634.

146. Leung PC, Harshey RM. 1991. Two mutations of phage Mu transposase that affect strand transfer or interactions with B protein lie in distinct polypeptide domains. *J Mol Biol* **219:**189–199.

Author Queries

Q1: For Figure 5 please give the reference number or full reference details for the source illustration. If the source article for A is not the same as that for B, please place both at the end of the legend with '(A)' inserted after the first and '(B)' after the second.

Q2: For Figure 7, the permission details are placed at the end of the legend as required by the style. Please check these are given appropriately, and confirm permission to reproduce these has been obtained from the publishers of references 85 and 106 (or confirm that permission is not required as you are an author).

Q3: For Figure 8, the permission details are placed at the end of the legend as required by the style. Please check these are given appropriately, and confirm permission to reproduce these has been obtained from the publishers of reference 34 (or confirm that permission is not required if you are an author).